THESIS FOR THE DEGREE OF DOCTOR OF PHILOSOPHY

The interaction of dissolved hydrogen with α-radiolytic oxidants during nuclear fuel dissolution

LOVISA BAUHN

Department of Chemistry and Chemical Engineering

CHALMERS UNIVERSITY OF TECHNOLOGY

Gothenburg, Sweden 2017

The interaction of dissolved hydrogen with α-radiolytic oxidants during nuclear fuel dissolution
LOVISA BAUHN
ISBN 978-91-7597-580-1

Doktorsavhandlingar vid Chalmers tekniska högskola
Ny serie nr 4261
ISSN 0346-718X

Nuclear Chemistry
Department of Chemistry and Chemical Engineering
Chalmers University of Technology
SE-412 96 Gothenburg
Sweden
Telephone + 46 (0)31-772 1000

Cover: Autoclaves used in the radiolysis experiments

Chalmers Reproservice
Gothenburg, Sweden 2017

The interaction of dissolved hydrogen with α-radiolytic oxidants during nuclear fuel dissolution

LOVISA BAUHN

Nuclear Chemistry
Department of Chemistry and Chemical Engineering
Chalmers University of Technology

ABSTRACT

Used nuclear fuel contains radiotoxic elements that will need to be kept isolated from the biosphere over a time period of 100 000 years. The KBS-3 geological storage concept aims to prevent the migration of radionuclides into the environment by different engineered barriers. As a complement to these engineered barriers, the low solubility of UO_2 in water will limit the release of radiotoxic elements from the fuel in the event of groundwater intrusion. However, the strong radiation field from the used fuel will result in radiolysis of any intruding water, creating H_2O_2 and other oxidative species. Although radiolytic oxidants have the ability to alter UO_2 dissolution behaviour, hydrogen gas formed in the anoxic corrosion of iron in the canisters has been shown to protect the fuel from radiation-induced dissolution.

In this research, the interaction of dissolved hydrogen with oxidants produced in the radiolysis of water subjected to α-radiation was studied. The studies were performed experimentally by means of homogeneous α-radiolysis, as well as leaching of SIMFUEL and a high activity MOX fuel. The possible inhibition of the hydrogen effect by the presence of bromide in groundwater was also investigated. Preparations for the studies included oxidation and neutralization of a ^{238}Pu solution, as well as method development for low concentration oxygen measurements by gas mass spectrometry.

The results suggest that the presence of dissolved bromide does not affect the production of α-radiolytic oxidants. It was further shown that the consumption of α-radiolytic oxidants by hydrogen does not occur in the bulk solution, which confirms the role of fuel surfaces in the activation of hydrogen. In the leaching of SIMFUEL in water with added H_2O_2, only 0.02% of the H_2O_2 consumption could be related to fuel dissolution by oxidation of uranium, while the main part was shown to decompose on the fuel surface. Formation of semi-heavy water (HDO) during leaching in a deuterium atmosphere indicated that a reaction may occur between dissolved hydrogen and hydroxyl radicals from the hydrogen peroxide decomposition. It was also shown that the protective effect of hydrogen on the radiation-induced dissolution of the fuel is maintained even at α-activities comparable to those of fresh spent fuel.

Keywords: α-radiolysis, gas mass spectrometry, hydrogen effect, bromide, SIMFUEL, MOX

List of Publications

This thesis is based on the work contained in the following papers:

I. Fleischer, S., Bauhn, L., Fors, P., Ödegaard-Jensen, A. (2013) Dark oxidation of water in soils. *Tellus B*, vol. 65, issue 1, article 20490.

Contribution: Method development and data evaluation of oxygen measurements.

II. Bauhn, L., Ekberg, C., Fors, P., Spahiu, K. (2017) The effect of bromide on oxygen yields in homogeneous α-radiolysis. *MRS Advances*, vol. 2, issue 13, pp. 711-716.

Contribution: Main author, all experimental work and data evaluation.

III. Bauhn, L., Hansson, N., Ekberg, C., Fors, P., Spahiu, K. The fate of hydroxyl radicals produced during H_2O_2 decomposition on a SIMFUEL surface in the presence of dissolved hydrogen. Manuscript.

Contribution: Part of manuscript writing, all experimental work and data evaluation.

IV. Bauhn, L., Hansson, N., Ekberg, C., Fors, P., Delville, R., Schuurmans, P., Verwerft, M., Spahiu, K. The interaction of molecular hydrogen with α-radiolytic oxidants on a $(U,Pu)O_2$ surface. Manuscript.

Contribution: Part of manuscript writing, experimental work and data evaluation.

Table of Contents

1. Introduction

Nuclear power is presently a major source of electricity in many countries of the world. In 2015, a total of 441 reactor units around the world supplied over 2 400 TWh electricity [1], corresponding to approximately 10% of world consumption [2]. Although offering an option for electricity production with very low carbon dioxide emissions, the technique has been questioned since its introduction in the 1950s on the basis of safety, its connection with nuclear weapons and the creation of long-lived radiotoxic waste. The future of nuclear power has thus been a much-disputed issue and the subject of many political debates in which different options ranging from immediate decommissioning to the development of a new generation reactor systems have been argued for. Regardless of the outcome of such discussions, the fact remains that a safe disposal for the accumulated used nuclear fuel from past and present electricity production will be necessary.

In Sweden, a geological repository is planned in which the fuel will be buried in copper canisters 500 metres deep in the granitic bedrock [3, 4]. An application for permission to construct the repository was submitted to the authorities in 2011 and is currently under review. Due to the radiotoxic and long-lived nature of many of the elements in used nuclear fuel, the requirements on the repository with regards to safety and durability are very high.

The repository is designed to prevent contact between the fuel and the groundwater, which could otherwise facilitate migration of radiotoxic elements to the environment. Nevertheless, scenarios of groundwater intrusion due to failure of the protective barriers, such as canister corrosion, are being investigated as part of the safety assessment [5, 6].

In its initial form the fuel has a very low solubility in water, a property that has resulted in the fuel matrix itself being considered a barrier against radionuclide migration. Oxidative species created through radiolysis of water in the vicinity of the fuel could however alter its dissolution behaviour. The presence in the groundwater of dissolved species could also have effects on the fuel dissolution through complexation of oxidized fuel elements or competing interactions with radiolysis products.

Radioactive decay causes the composition of the used fuel to change over time. After a few hundred years of storage short-lived species will have decayed and the radiation field from the fuel will be dominated by α-radiation from the long-lived actinides [7]. Groundwater intrusion at this stage would thus result in high yields of α-radiolytic products, of which hydrogen peroxide is one of the main oxidants [8]. The intrusion of groundwater would also result in a build-up of significant amounts of molecular hydrogen due to anoxic corrosion of canister iron [9]. By interaction with radiolytically formed oxidants, the presence of dissolved hydrogen in the water has been shown to have a protective effect on the radiation-induced dissolution of used nuclear fuel [10, 11].

The highly radioactive nature of used nuclear fuel limits the possibilities for experimental research. In addition, aged used fuel does not yet exist. For these reasons, much of the research within this area is based on un-irradiated fuel or low-active surrogates for used fuel. Experiments have also been made using external irradiation, or with α-doped materials simulating used fuel of a certain age with respect to α-activity. By these types of experimental simulations different mechanisms of the radiation-induced dissolution can be isolated and studied separately.

In this work, the interaction between dissolved hydrogen and oxidants produced in α-radiolysis of water has been studied by means of homogeneous radiolysis experiments, as well as leaching of different UO_2-based materials under repository conditions. The possible inhibition of the hydrogen effect during α-radiolysis by the presence of bromide in the groundwater has also been investigated. Preparations for the experimental studies have included

method development for mass spectrometric measurements of low concentration oxygen gas, as well as the preparation of a high activity ^{238}Pu solution at neutral pH for the purpose of radiolysis experiments under groundwater conditions with an evenly distributed α-dose.

2. Background

In the employment of nuclear power throughout the world different concepts have been chosen with regard to reactor designs, fuel types and waste management options. This chapter presents a background to the project, with a main focus on the current situation in Sweden.

2.1. Nuclear fuel

Sweden presently has nine nuclear reactors in operation, all of which are light water cooled and moderated reactors of the type BWR (boiling water reactor) or PWR (pressurized water reactor). Both types are operated with uranium dioxide fuel in the form of sintered pellets.

Uranium exists in nature as a radioactive primordial element, and has been present since the formation of the earth. In its natural form uranium consists of three isotopes; 0.0055% ^{234}U, 0.7200% ^{235}U and 99.2745% ^{238}U [12]. The uranium used for light water reactor fuel is typically enriched to 3-5% with respect to its fissile isotope ^{235}U.

2.1.1. Nuclear reactions in the reactor core

During reactor operation fission is induced in the ^{235}U nuclei by neutron absorption, resulting in the formation of two fission products and two to three neutrons per fission event. The release of neutrons thus facilitates a chain reaction in the core of the reactor that is maintained and controlled by the use of neutron absorbers. Each fission event is associated with the release of approximately 200 MeV energy, of which the main part is kinetic energy of the fission fragments [13].

In addition to fission products there is also a build-up of heavier elements in the fuel caused by neutron capture in the much more abundant isotope ^{238}U. Successive neutron absorptions, followed by radioactive decay, result in the formation of different isotopes of uranium, plutonium and minor actinides. The formation of ^{239}Pu by reaction 2.1 adds to the fissile content of the fuel, as does the formation of ^{241}Pu by further neutron capture. This means that the heat produced in the reactor originates not only from the fission of uranium but also from the fission of plutonium.

$$^{238}U(n,\gamma)^{239}U \xrightarrow{\beta^-} {}^{239}Np \xrightarrow{\beta^-} {}^{239}Pu \tag{2.1}$$

The splitting of a ^{235}U or a ^{239}Pu nucleus by thermal neutrons yields fission products within the mass range 65 to 170 atomic mass units. The statistical distribution of these yields show two peaks around mass units 95 and 135 for the fission of ^{235}U, with a slight distortion to higher mass units for the case of ^{239}Pu fission [14]. As many of the fission products initially formed are unstable, the composition of the fuel is transformed further by radioactive decay. Some fission products have extraordinary high probabilities for neutron absorption and are therefore commonly referred to as neutron poisons. As these elements accumulate in the fuel the neutron economy in the core is disturbed until finally a point is reached where the fission chain reaction can no longer be sustained. For this reason, the lifetime of a fuel element in the reactor core is limited to a few years.

At the end of reactor operation the fuel thus contains fission products, actinides and decay products in different amounts, depending on burn-up. The bulk part of the fuel however still consists of uranium dioxide.

2.1.2. Composition of used nuclear fuel

In addition to the changes on the atomic level that occur during reactor operation, the fuel will be subject to structural alterations. Chemically the fission products present in used fuel can be divided into four groups; fission gases and volatile elements, metallic precipitates, ceramic precipitates, and elements dissolved as oxides in the fuel matrix [15]. The most common fission products listed in their respective groups are shown in Table 1. As is evident from the table, some elements can belong to different groups, and transitions between groups can occur as the fission processes proceed.

The metallic precipitates of the second group, also referred to as ε-particles, are of special interest in the context of used fuel corrosion, as described further in Chapter 3.

Table 1. Fission products divided into groups according to chemical state [15].

Group	Fission products
1) Fission gases and volatile elements	Kr, Xe, Br, I
2) Metallic precipitates	Mo, Tc, Ru, Rh, Pd, Ag, Cd, In, Sn, Sb, Te
3) Ceramic precipitates	Rb, Cs, Ba, Zr, Nb, Mo, Te
4) Oxides dissolved in the fuel	Sr, Zr, Nb, Y, La, Ce, Pr, Nd, Pm, Sm

2.1.3. Radiotoxicity of nuclear fuel

Radiotoxicity is a measure of the possible damage caused by ingestion or inhalation of radioactive substances, usually expressed as radiation dose per unit of intake. Although uranium itself is radioactive the radiation dose from the fuel to its surroundings is increased by many orders of magnitude during reactor operation. As described in the previous sections, the nuclear reactions occurring within the core of a reactor result in the formation of actinides, fission products and decay products in different forms, many of which are highly radiotoxic.

The change in used fuel radiotoxicity over time can be calculated based on its original composition at the time of removal from the reactor and the half-lives of the different nuclides and their daughters. The result of one such calculation is shown in Figure 1, with the reference level corresponding to the amount of natural uranium used for the production of one tonne of enriched fuel. As seen in the graph, the relatively short-lived fission products decay within the first few hundred years, after which the long-lived actinides provide the largest contribution to the total radiotoxicity. The reference level is reached after approximately 100 000 years, illustrating the time perspective over which safe storage of the used nuclear fuel will be necessary.

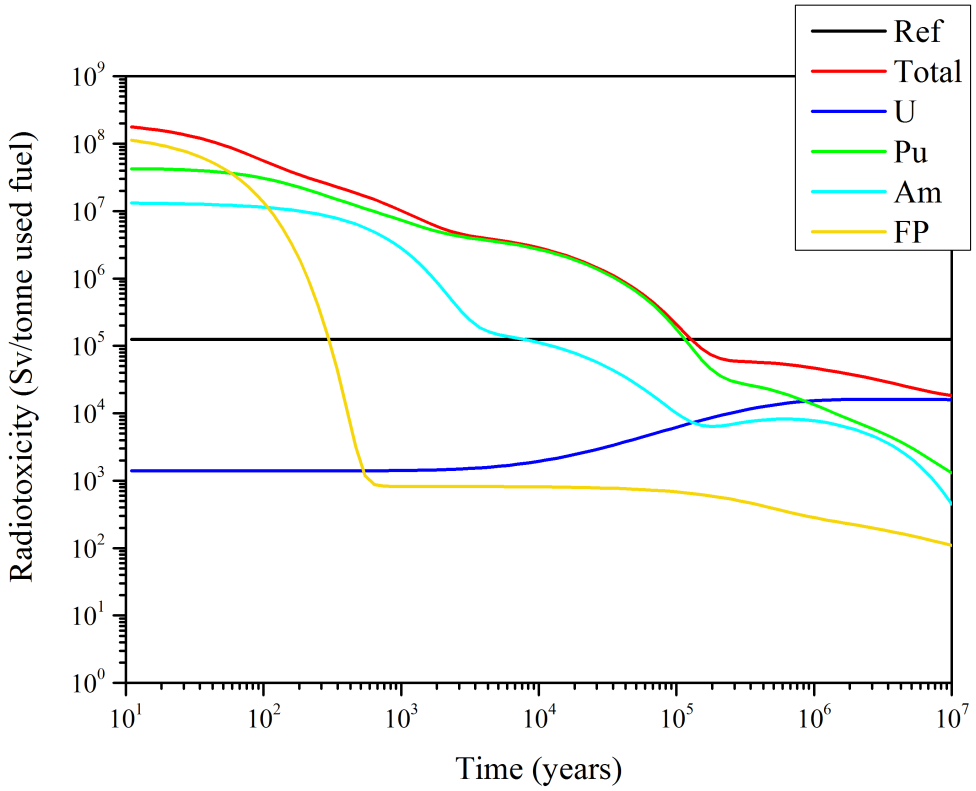

Figure 1. Radiotoxicity of used nuclear fuel over time. Calculation from RadTox [16] based on UOX fuel with 4% enrichment, 45 GWd/tIHM burnup and 10 y cooling time.

2.2. Management of radioactive waste

Radioactive waste is generated mainly within the nuclear power industry, but also to some extent from other sources, such as medical diagnostics and treatments, as well as various research applications. Historically, quite significant amounts of nuclear waste have also been accumulated in some countries as a result of military activities. The methods of waste treatment and storage options differ between countries, as does the decisions on where the responsibility for the nuclear waste management lies. In Sweden the producers of electricity are obligated to take care of the nuclear waste generated in connection with power production, including the used nuclear fuel.

2.2.1. Classification

The requirements for nuclear waste treatment or storage depend on the activity level of the waste, as well as the half-life of the elements present in the waste. According to international safety standards [17], the following six classes of radioactive waste are identified:

1) Exempt waste (EW)
2) Very short-lived waste (VSLW)
3) Very low level waste (VLLW)
4) Low level waste (LLW)
5) Intermediate level waste (ILW)
6) High level waste (HLW)

Any waste with an activity below a certain clearance level is considered exempt waste and does not require any regulatory control [17]. The second category includes waste which due to very short half-life reaches the clearance level within a few years and thus only needs short-time isolation.

Low and intermediate level waste on the other hand needs to be isolated and contained in dedicated storage facilities. It does not however require cooling. In Sweden, short-lived low and intermediate level waste is stored in SFR (final repository for short-lived radioactive waste), which has been in operation since 1988. The repository contains operational waste from Swedish nuclear power plants, as well as hospitals and research facilities. In addition to its current capacity of 63 000 m^3, an extension of the repository is planned in order to facilitate the storage of decommissioning waste. Some of the waste will be stored in a separate facility due to its long half-life. This facility is called SFL (final repository for long-lived radioactive waste), and has yet to be constructed.

Used nuclear fuel is categorized as high level waste because of its high activity levels and very long life-time. The heat generation from the fuel also imposes special requirements on its storage.

2.2.2. Interim storage

In Sweden the so called once-through fuel cycle has been chosen, meaning that there is no reprocessing or recycling of the used fuel. Following reactor operation the fuel is stored at the nuclear power plant and then transported to an interim storage facility (CLAB) where it is kept in deep storage pools. The water in the pools provides radiation protection, as well as cooling of the residual decay heat from the fuel.

After cooling at the interim storage facility the fuel is ready for final storage. Since the geological repository is not yet in operation, all used fuel produced in Sweden since the introduction of nuclear power is currently stored at CLAB. As of 2016 the total amount was 6 500 tonnes [18].

2.2.3. Final repository

Construction of a final repository, together with an encapsulation plant for the used fuel, is planned to commence during the early 2020s. The KBS-3 concept for storage of used nuclear fuel is based on different barriers designed to protect the environment from any effects of the radiotoxic waste. As shown in Figure 2, the barriers include copper canisters enclosing the fuel bundles, bentonite clay filling the space between the canisters and the inner walls of the boreholes, and the granitic bedrock in which the canisters will be buried. The five-centimetre-thick copper canisters with cast iron inserts are designed to withstand corrosion and geological movements. The bentonite clay is a water-absorbing buffer that provides further protection from movements in the bedrock, whilst also functioning as a two-way sorption barrier for water-soluble species. If there is groundwater intrusion the bentonite clay can thus restrict migration of radionuclides, as well as prevent corrosive species from entering the system.

Due to the extensive timescale to be considered in the safety assessment of a final repository, contact between fuel and groundwater cannot be disregarded. In such a scenario the migration of radiotoxic elements with the groundwater to the environment will be limited by their retention within the fuel matrix. Much research has therefore been dedicated to the radiation-induced oxidative dissolution of uranium dioxide, in which its dissolution behaviour is altered by oxidants produced in the radiolysis of water. Furthermore, groundwater intrusion will result in the formation of significant amounts of hydrogen from anoxic corrosion of the canister iron.

Although the exact mechanisms are not yet fully elucidated, it is clear that hydrogen has a protective effect on radiation-induced dissolution of the fuel.

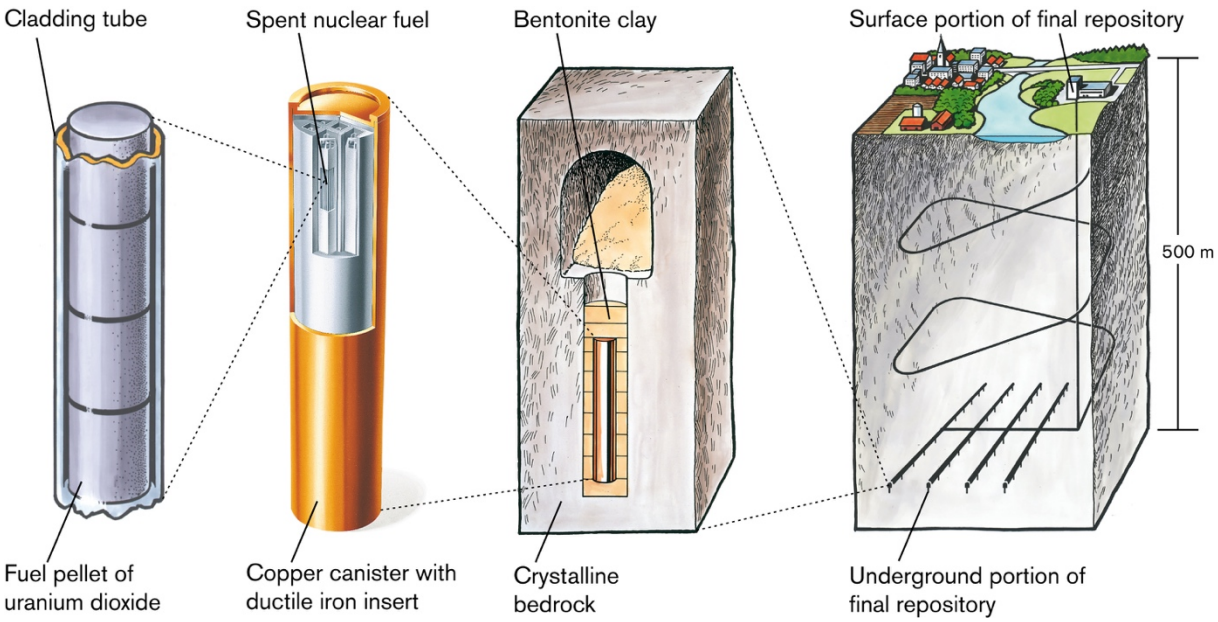

Figure 2. The different barriers of the geological repository according to the KBS-3 method. Source: Svensk Kärnbränslehantering AB. Illustrator: Jan M Rojmar.

2.3. Radiolysis and fuel corrosion studies

As mentioned in the introduction, the possibilities for experimental studies of spent fuel corrosion are limited, with one of the complicating factors being its inherent high activity. Furthermore, although spent fuel can be handled at designated research facilities, none of the existing spent fuel in the world is older than 70 years, which means that its composition is not representative of spent fuel after thousands of years in storage. To circumvent these issues, and to isolate effects of different mechanisms, fuel corrosion research includes the combination of several different approaches.

2.3.1. External irradiation

In radiolysis experiments featuring external irradiation, radioactive sources or accelerators can be used. In this way radiolysis yields from different types of radiation can be effectively studied without interference of other factors, such as fuel surfaces or mixed radiation fields. Studies have also been performed on fuel-water systems subjected to external irradiation. For the case of α-radiolysis this has for example been done by close positioning of a UO_2 pellet from an α-source so that the pellet is within range of the α-particles in water [19].

2.3.2. Homogeneous radiolysis

Another option for studying radiolysis reactions in the absence of a fuel surface is homogeneous radiolysis, in which the radiation-emitting substance is dissolved in the solution. The advantage of this type of experiment is a uniform distribution of the radiation dose to the water. For α-

radiolysis studies this approach can be beneficial considering that the range of α-particles in water is only about 40 μm. The volume in which the dose from an external source is deposited is thus very small, and could lead to misinterpretations of the results.

Appropriate α-emitters for homogeneous radiolysis can be selected based on half-life, decay chain and solubility. If β- or γ-radiation is to be avoided the choice of nuclide is further limited. One suitable option is ^{238}Pu, which decays to ^{234}U with no significant γ-emission. Its half-life of 88 years is sufficiently short so that a high dose is delivered to the water even at relatively low Pu concentrations, while long enough so that the dose rate can be considered constant over the time of experiment. Furthermore, since the half-life of the daughter nuclide is $2.5 \cdot 10^5$ years, no further decays need to be considered. However, plutonium does have a limited solubility in water, which needs to be taken into account in the experimental design.

2.3.3. Leaching

Fuel leaching studies involve the contact between fuel material and water, typically with monitoring of the concentration of uranium (and possibly other elements) in the leachate solution. The fact that the release of radionuclides from used fuel is governed by dissolution of the UO_2 matrix means that leaching of pure UO_2 can provide relevant information for safety assessments. Numerous studies have therefore been performed on the leaching of UO_2 pellets, as well as on powder suspensions.

There are also different types of simulated used fuel, fabricated for research purposes. SIMFUEL refers to UO_2 material with additions of Sr, Y, Zr, Mo, Ru, Rh, Pd, Ba, La, Ce and Nd as inactive substitutes for fission products. These represent the fission products that form metallic or ceramic precipitates in the fuel or exist as oxides dissolved in the fuel, i.e. they belong to groups 2 through 4 in Table 1. The advantage of SIMFUEL is that effects on the dissolution behaviour due to chemical and structural changes of the fuel from fission processes can be studied without the inconvenience of handling highly radioactive materials. Another type of used fuel imitation is α-doped fuel, which is a simulation of aged used fuel with respect to α-activity. This is usually made from natural or depleted uranium doped with an α-emitter of higher specific activity, such as ^{233}U or Pu. Depending on the type and amount of dopant, fuel pellets with α-activity corresponding to used fuel of different ages can be fabricated.

Finally, leaching experiments are also conducted using actual spent fuel. Although these types of experiments are inherently more complicated, they are a necessary piece of the puzzle in the understanding of radiation-induced oxidative dissolution.

3. Theory

In this chapter the theory of gas mass spectrometry is briefly presented. The solution chemistry of plutonium is also discussed, as a basis for the Pu work included in the homogeneous radiolysis studies. Finally, the theoretical basis for radiolytically driven oxidative dissolution of used nuclear fuel is presented.

3.1. Gas mass spectrometry

Measurement of gas composition by mass spectrometry is based on ionization of the gas, followed by detection of the ions based on their mass-to-charge ratio. The functioning of the mass spectrometer can thus be described in three main steps: ionization, separation and detection.

3.1.1. Ionization

The ion source contains a filament (Re, W or Y_2O_3/Ir) that emits electrons upon heating. During acceleration through a formation space containing the sample gas, the electrons collide with gas molecules, creating single- or multiple-charge ions. The ion yield varies with the type of gas and applied voltage. A maximum yield is normally achieved with electron energies between 70 and 100 eV. Fragmentation and recombination of ionized molecules occur in the ion source, and this needs to be taken into account in the evaluation of data.

3.1.2. Separation

The characteristics of a gas mass spectrometer are to some extent defined by its type of mass filter. In a quadrupole mass spectrometer, alternating quadrupolar electric fields are used to separate ions according to their mass-to-charge ratios. The mass filter system consists of two pairs of cylindrical rods placed in parallel, as shown in Figure 3. When voltages are applied between the rods the ionized gas molecules are deflected in the electric field that is created.

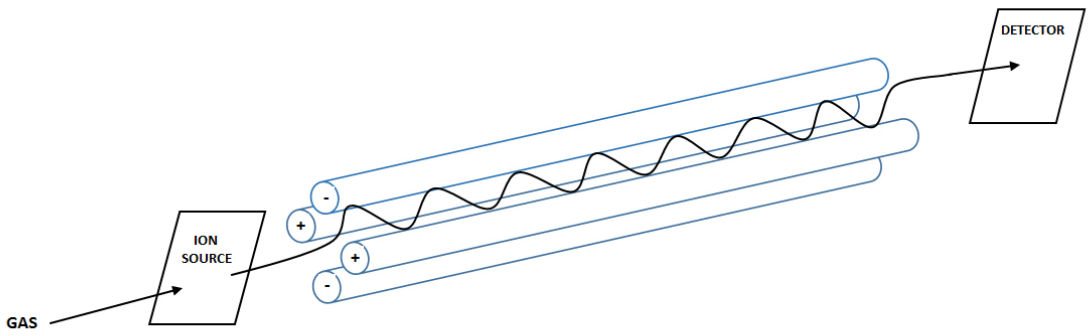

Figure 3. Simplified schematics of a quadrupole gas mass spectrometer.

The deflection of an ion by a given voltage can be derived from its equations of motion in the x- and y-direction. If the amplitude of its helical trajectory exceeds the field radius the ion is discharged and does not reach the detector. If the amplitude is lower the ion reaches the detector and is counted. By scanning over a range of voltages, multiple ions can be detected during the same measurement.

3.1.3. Detection

The ion current from a gas component is directly proportional to the partial pressure of the gas component in the sample. For measurements of very low ion currents a secondary electron multiplier (SEM) detector, or a continuous secondary electron multiplier (C-SEM) detector, is most suitable, as the multiplication of electrons gives an increased sensitivity. The high signal-to-noise ratio also gives very low detection limits. The SEM contains multiple stages of dynodes connected in series. At the impact of an ion or electron, secondary electrons are generated on each dynode, thus creating an avalanche of electrons from each detected ion. A C-SEM consists of one conversion dynode followed by a glass tube on the inside of which the electron avalanche is created. However, the dynodes are sensitive to contamination, which can alter the multiplication factor. This factor is also dependent on the energy of the incoming ion, which means that gas-specific calibration is important.

3.2. Plutonium solution chemistry

The complexity of plutonium chemistry is a consequence of its many possible oxidation states. In aqueous solution the behaviour of plutonium is governed by its redox chemistry and its tendency towards hydrolysis and colloid formation, as well as complexation with other ligands.

3.2.1. Redox chemistry

In acidic solution the tri- and tetravalent states are the most stable, and these exist as positively charged hydrated aquo ions [20]. Plutonium in the penta- and hexavalent states exists as the trans-dioxo cations PuO_2^+ and PuO_2^{2+}, more commonly known as plutonyl ions [20]. These states become more stable as pH increases [21].

Heptavalent plutonium has been prepared by ozone oxidation of Pu(VI) [22], but it is only stable under highly alkaline conditions in the presence of an oxidizing agent. Recent studies have confirmed the existence of Pu(VII) in its tetraoxo-monoanionic form PuO_4^-, which hydrolyses to the tetraoxo-dihydroxo anion $[PuO_4(OH)_2]^{3-}$, and spontaneously reduces to Pu(VI) with a half-life of 3.7 hours [23]. There have also been suggestions of a partial formation of Pu(VIII) during the preparation of Pu(VII) by ozonisation in alkaline solutions [24-27].

In acidic solutions without complexing agents Pu(IV) will undergo disproportionation according to reaction 3.1 [20].

$$3Pu^{4+} + 2H_2O \rightleftarrows 2Pu^{3+} + PuO_2^{2+} + 4H^+ \qquad (3.1)$$

As evident from the fourth order dependence on hydrogen ion concentration, there will be little or no disproportionation of Pu(IV) in highly acidic solutions. It should also be noted that the concentration of Pu(IV), and thus the equilibrium constant, will be affected by hydrolysis, as well as plutonium self-reduction by α-radiolysis [28].

Evidence of the disproportionation of pentavalent plutonium was first found during Raman spectroscopy studies of a PuO_2^+ solution [29]. This disproportionation results in the formation

of Pu(VI) and Pu(III) or Pu(IV) by reactions 3.2 and 3.3, respectively [20]. Either one of the reactions can be predominant, depending on solution conditions.

$$3PuO_2^+ + 4H^+ \rightleftarrows Pu^{3+} + 2PuO_2^{2+} + 2H_2O \quad (3.2)$$

$$2PuO_2^+ + 4H^+ \rightleftarrows Pu^{4+} + PuO_2^{2+} + 2H_2O \quad (3.3)$$

3.2.2. Solubility

PuO_2 can be dissolved in acidic solutions. However, the solubility becomes limited already at pH 1 by the extensive hydrolysis of Pu^{4+} and the low solubility of the hydroxides thereby formed. Although hydrolysis of plutonium in other oxidation states does occur, it is the formation and precipitation of tetravalent plutonium hydroxide that are considered to be the solubility limiting processes.

Plutonium colloids are large polynuclear hydroxides that form with increasing hydrolysis and can stay suspended in solution up to sizes of approximately 10 nm without precipitating. The formation of colloids can thus seem to increase the solubility of plutonium, a phenomenon which possibly has led to misinterpretations of plutonium solubility data in the past. More thorough investigations of the connections between plutonium(IV) concentration and colloid formation have therefore been conducted [30, 31]. In recent studies of colloid formation small polymers of mixed oxidation states have been observed [32]. Another interesting finding on this topic is that aging colloids seem to decrease in size [33].

Formation of plutonium hydroxide by hydrolysis proceeds according to the following reaction [34], where the case of $p = 1$ represents the formation of mononuclear hydroxides.

$$pPu^{4+} + qH_2O \rightleftarrows Pu_p(OH)_q^{4p-q} + qH^+ \quad (3.4)$$

The formation of mononuclear plutonium hydroxide species can thus be described stepwise by the following reactions:

$$Pu^{4+} + OH^- \rightleftarrows PuOH^{3+} \quad (3.5)$$

$$PuOH^{3+} + OH^- \rightleftarrows Pu(OH)_2^{2+} \quad (3.6)$$

$$Pu(OH)_2^{2+} + OH^- \rightleftarrows Pu(OH)_3^+ \quad (3.7)$$

$$Pu(OH)_3^+ + OH^- \rightleftarrows Pu(OH)_4 \quad (3.8)$$

The formation constants for each hydrolysed species are then given by equation 3.9, where the index $1q$ denotes a mononuclear complex formed in hydrolysis step q.

$$\beta_{1q} = \frac{\{Pu(OH)_q^{4-q}\}}{\{Pu^{4+}\}\{OH^-\}^q} \ , q = 1,..,4 \quad (3.9)$$

For crystalline plutonium dioxide, dissolution or precipitation is described by the equilibrium reaction

$$PuO_2(s) + 2H_2O \rightleftarrows Pu^{4+} + 4OH^- \quad (3.10)$$

Tetravalent plutonium can also precipitate as an amorphous hydrous oxide, $PuO_2 \cdot xH_2O$, or plutonium hydroxide, $Pu(OH)_4$. For the case of x = 2, these forms are stoichiometrically identical, and the fact that this solid phase is not well defined is thought to be one of the reasons for the wide variations in solubility data available in the literature [31]. In this case the dissolution proceeds according to the following reaction:

$$Pu(OH)_4 \rightleftarrows Pu^{4+} + 4OH^- \tag{3.11}$$

The solubility product for both the crystalline and the amorphous form can therefore be described by

$$K_{sp}^0 = \{Pu^{4+}\}\{OH^-\}^4 \tag{3.12}$$

The solubility for tetravalent plutonium can be estimated based on the dissolution reactions given above, and the stepwise hydrolysis as described in reactions 3.5 through 3.8. The result of one such calculation is shown in Figure 4 for the cases of crystalline and amorphous solid phases, under the assumption of ideal solution. The solubility products and hydrolysis formation constants used in the calculation are summarized in Table 2.

Table 2. Solubility products and hydrolysis constants used in the calculation of theoretical solubility of tetravalent plutonium. All data from Neck and Kim [30].

Solid phase	**log K_{sp}**
PuO_2 (cr)	-64.1 ± 0.7
$PuO_2 \cdot xH_2O$ (am)	-58.5 ± 0.7
Hydrolysis species	**log β_{1q}**
$Pu(OH)^{3+}$	14.6 ± 0.2
$Pu(OH)_2^{2+}$	28.6 ± 0.3
$Pu(OH)_3^{+}$	39.7 ± 0.4
$Pu(OH)_4(aq)$	48.1 ± 0.9

As evident from the graphs in Figure 4, there is a rapid decrease of solubility with decreasing acidity and although the amorphous form is more soluble by orders of magnitude compared to the crystalline form, its solubility is still only in the range of 10^{-10} M at neutral pH.

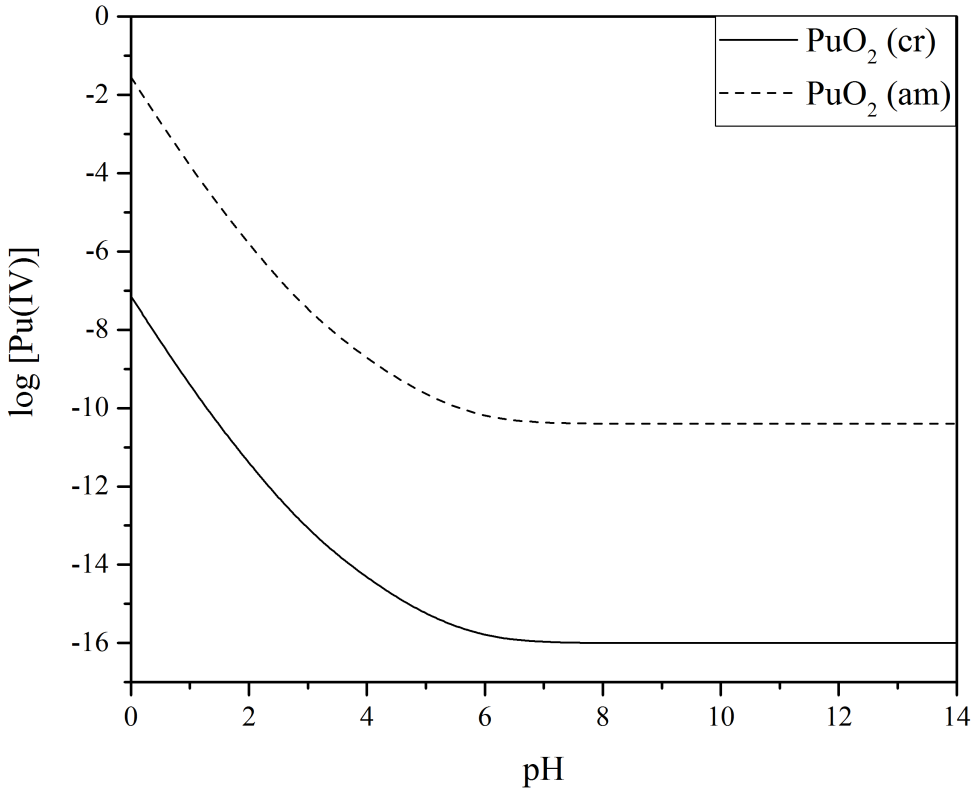

Figure 4. Theoretical solubility at zero ionic strength of crystalline and amorphous PuO_2. The calculation is based on data from Neck and Kiim [30]

.

3.2.3. Complexation

In non-complexing aqueous media, water molecules are coordinated around the plutonium atoms, forming positively charged aquo ions. The number of water molecules associated with each metal atom can vary depending on the ionic strength [35]. Tri- and tetravalent plutonium aquo ions commonly include eight or nine water molecules, which gives a number of possible molecular geometries, such as the square antiprism, the dodecahedron, or the tricapped trigonal prism. Since the penta- and hexavalent forms of plutonium exist as linear plutonyl ions, the coordination of water molecules is in these cases limited to the equatorial plane, and the most common geometry is a pentagonal bipyramid with five water molecules [35].

In complex formation the ligands can change places with one or more of the coordinated water molecules of the aquo ions and thereby form inner sphere complexes. Depending on ionic strength of the solution, formation of the weaker outer sphere complexes can also occur [20].

In general, plutonium ions are known to form stable complexes with oxoanions, in particular the phosphate ion, PO_4^{3-} [20]. However, the most well-known ligands in plutonium chemistry are probably the nitrate and carbonate ions, due to their respective associations with plutonium separation chemistry and environmental chemistry. Out of these two ligands, carbonate forms the stronger complexes.

The stability of plutonium(VI) carbonate complexes has been of particular interest from an environmental point of view, since the presence of carbonate in groundwater could potentially

increase the mobility of plutonium [36]. Several studies have therefore been dedicated to the solubility of PuO_2CO_3(s) [37-39].

3.3. Radiolysis of water

In the interaction of ionizing radiation with water, radiolysis products are formed in the chain reactions initiated by excitation or ionization of water molecules. Both oxidizing and reducing species are formed, and their respective yields are to some extent dependent on radiation type and energy.

3.3.1. Radiolysis reactions

The radiolysis reactions proceed in what is usually described as different stages, referring to the different timescales over which the reactions occur. Ionization or excitation of water molecules occurs within 10^{-16} seconds following the absorption of energy, corresponding to the time of an electronic transition. This first stage is therefore referred to as the physical stage.

Within 10^{-14} seconds after radiation absorption, the ionized water molecules will react with the surrounding water to form hydroxyl radicals and hydronium ions, according to reaction 3.13.

$$H_2O^+ + H_2O \rightarrow \cdot OH + H_3O^+ \tag{3.13}$$

The free electrons from the water ionizations will reach thermal equilibrium with the water within 10^{-12} seconds. If sufficiently high, the energy released during this process can cause further ionizations or excitations. Together with the dissociation of excited water molecules, on a timescale corresponding to a molecular vibration, this is referred to as the physicochemical stage. In the dissociations, radicals are formed together with molecular hydrogen, according to reactions 3.14 and 3.15.

$$H_2O^* \rightarrow H\cdot + \cdot OH \tag{3.14}$$

$$H_2O^* \rightarrow H_2 + O\cdot \tag{3.15}$$

The chemical stage of the radiolysis occurs at 10^{-12} to 10^{-7} seconds after radiation absorption, and includes recombination of the radicals formed in equations 3.13 through 3.15, as well as diffusion of radiolysis products to the bulk water. The recombination reactions result in the formation of molecular products or secondary radicals, as shown in the following reactions [40]:

$$e^-_{aq} + e^-_{aq} + 2H_2O \rightarrow H_2 + 2OH^- \tag{3.16}$$

$$e^-_{aq} + \cdot OH \rightarrow OH^- \tag{3.17}$$

$$e^-_{aq} + H_3O^+ \rightarrow H\cdot + H_2O \tag{3.18}$$

$$e^-_{aq} + H\cdot + H_2O \rightarrow H_2 + OH^- \tag{3.19}$$

$$H\cdot + H\cdot \rightarrow H_2 \tag{3.20}$$

$$\cdot OH + \cdot OH \rightarrow H_2O_2 \quad (3.21)$$

$$\cdot OH + H \cdot \rightarrow H_2O \quad (3.22)$$

$$H_3O^+ + OH^- \rightarrow 2H_2O \quad (3.23)$$

3.3.2. Radiolysis yields

The primary yields of water radiolysis are commonly referred to as G values and are expressed in units of amount of product formed per absorbed energy. The yields include both radicals and molecular products resulting from the chemical stage of radiolysis. In oxygen-free water, these products are e^-_{aq}, H·, ·OH, H_2, H_2O_2 and H_3O^+ [40]. The formation of oxygen gas is related to water radiolysis through the decomposition of hydrogen peroxide, according to reaction 3.24.

$$2H_2O_2 \rightarrow O_2 + 2H_2O \quad (3.24)$$

Additional oxidants can be formed in the reactions between oxygen and solvated electrons or hydrogen radicals [40]:

$$e^-_{aq} + O_2 \rightarrow O_2 \cdot^- \quad (3.25)$$

$$H \cdot + O_2 \rightarrow HO_2 \cdot \quad (3.26)$$

The variation of yields with radiation type and energy is an effect of differences in range, or linear energy transfer (LET). The characteristics of α-radiation are very short range and high LET, which means that its energy is absorbed in a very small volume of the irradiated material. In water radiolysis the effect of high LET is a close radiation track formation with high density of radicals, which increases the possibilities for recombination reactions. Therefore α-radiolysis gives relatively high yields of molecular products. β- or γ-radiation, on the other hand, has longer range and lower LET values, resulting in higher fractions of radical diffusion to the bulk water.

3.4. Fuel dissolution

Migration of radiotoxic elements from used nuclear fuel to the biosphere is reliant on groundwater transport and is therefore limited by dissolution rates. The fission products, actinides and decay products are embedded in the UO_2 matrix, which constitutes approximately 95% of the used fuel. The release of these nuclides is thereby restricted by the dissolution rate of UO_2.

3.4.1. Solubility of UO_2

In stoichiometric UO_2, uranium is present in its tetravalent form and has a very limited solubility in water. Analogous to the case of PuO_2 described in Chapter 3.2, its solubility is partly determined by the degree of crystallinity. Given the constants summarized in Table 3, a calculation equivalent to that described previously for PuO_2 shows that the theoretical solubility at neutral pH is $10^{-14.9}$ M for crystalline UO_2 and $10^{-8.5}$ M for amorphous UO_2.

When subjected to air UO_2 is prone to superficial oxidation, resulting in the formation of a UO_{2+x} phase on the surface. Studies of radiation-induced dissolution are easily affected by the

higher solubility of this pre-oxidized layer and should therefore include treatments of the fuel material to restore the stoichiometry prior to leaching [41, 42]. Common pre-treatments include annealing and/or wash cycles in carbonate solution. Studies have shown that the extent of the surface oxidation depends not only on the time of air exposure but also on the α-activity [41].

Table 3. Solubility products and hydrolysis constants used in the calculation of theoretical solubility of tetravalent uranium. All data from [30].

Solid phase	**log K_{sp}**
UO_2 (cr)	-60.86 ± 0.36
$UO_2 \cdot xH_2O$ (am)	-54.5 ± 1.0
Hydrolysis species	**log β_{1q}**
$U(OH)^{3+}$	13.6 ± 0.2
$U(OH)_2^{2+}$	26.9 ± 1
$U(OH)_3^{+}$	37.3 ± 1
$U(OH)_4$(aq)	46.0 ± 1.4

3.4.2. Radiation-induced dissolution

Oxidative dissolution involves, as the name suggests, oxidation of a species to a more soluble form, followed by its dissolution. For the case of UO_2 the mechanism can be described by the oxidation reaction 3.27 and the dissolution reaction 3.28. When the oxidants involved in the oxidation reaction are the products of radiolysis, the process is referred to as radiation-induced dissolution.

$$UO_2(s) + ox \rightarrow UO_2^{2+}(s) + red \tag{3.27}$$

$$UO_2^{2+}(s) \rightarrow UO_2^{2+}(aq) \tag{3.28}$$

The oxidants formed in radiolysis include H_2O_2, O_2, ·OH, HO_2· and O_2·$^-$. If carbonate ions are present in the water their reaction with hydroxyl radicals (reaction 3.29) results in the formation of carbonate radical anions, which also have the ability to oxidize UO_2 [43].

$$HCO_3^- + \cdot OH \rightarrow CO_3 \cdot^- + H_2O \tag{3.29}$$

The presence of carbonate in the water also affects the UO_2 dissolution behaviour by complex formation with uranyl ions, thereby facilitating the release of oxidized uranium from the fuel surface [44].

Despite the high reactivity of radical species, it has been shown that it is the molecular oxidants that are the most important with respect to oxidative dissolution of UO_2, both in α- and γ-irradiated systems [43]. The mechanism for oxidation of UO_2 by H_2O_2 is given by the

two-step reaction 3.30 and 3.31, where the oxidation of U(IV) to U(V) is the rate limiting step [44].

$$UO_2(s) + H_2O_2 \rightarrow UO_2^+(s) + \cdot OH + OH^- \quad (3.30)$$

$$UO_2^+(s) + \cdot OH \rightarrow UO_2^{2+}(s) + OH^- \quad (3.31)$$

The oxidation of UO_2 by O_2 also involves a two-electron transfer in which the first step is rate determining. The reactivity of H_2O_2 towards UO_2 is however higher than that of O_2 by a factor of 200 [8].

3.4.3. The hydrogen effect

If there is groundwater intrusion into the repository significant amounts of hydrogen gas will be produced. The radiolysis of water is responsible for part of the hydrogen production through reactions 3.15, 3.16, 3.19 and 3.20. The main source of hydrogen however would be anoxic corrosion of the cast iron insert in the copper canisters containing the fuel, according to the following reactions:

$$Fe + 2H_2O \rightarrow Fe(OH)_2 + H_2 \quad (3.32)$$

$$3Fe + 4H_2O \rightarrow Fe_3O_4 + 4H_2 \quad (3.33)$$

Several studies have shown that the presence of dissolved hydrogen in the water protects the fuel from oxidative dissolution [10, 11, 42, 45-51]. These studies have involved leaching of different types of UO_2-based materials, including both simulated and actual spent fuel. However, the mechanisms of this hydrogen effect are not entirely identified.

By consumption of hydroxyl radicals, as shown in the equation below, molecular hydrogen can decrease the radiolytic formation of hydrogen peroxide (reaction 3.21).

$$H_2 + \cdot OH \rightarrow H_2O + H \cdot \quad (3.34)$$

Prevention of hydrogen peroxide production by this reaction is mainly relevant in the case of low LET radiation, where the radical yield is high. Radiolysis studies using external irradiation sources indicate that H_2 has little or no effect on H_2O_2 yields from α-radiation [52]. The discrepancy seen in the comparison between experimental results and theoretical modelling in this study was later clarified by adjusting the calculated radiation dose in accordance with the radiation absorbing volume [53].

Another explanation for the lower fuel dissolution rates observed in the presence of hydrogen could be reduction of the oxidized uranium, either on the fuel surface or in the bulk solution. The former option would prevent dissolution, while the latter would result in precipitation. Experiments with uranyl carbonate solutions [54] have shown that molecular hydrogen is capable of reducing dissolved U(VI) in the presence of a UO_2 surface. No such reduction occurred in the absence of UO_2, suggesting that hydrogen becomes activated on the UO_2 surface. The hydrogen activation on fuel surfaces has in many cases been accredited to the presence of ε-particles in the fuel. Nevertheless, although the presence of ε-particles may accelerate the hydrogen effect, evidence of hydrogen activation on UO_2 surfaces without these metallic inclusions has been demonstrated [50]. Interestingly, there have also been indications that the level of α-activity in the fuel may have some significance in relation to the hydrogen effect.

3.4.4. The bromide effect

The radiolysis scheme can also be influenced by elements naturally present in the groundwater. One such species is the bromide ion, which through its scavenging of hydroxyl radicals could inhibit the effect of hydrogen described in the previous section, thus counteracting the protective effect of hydrogen on the radiation-induced dissolution of the fuel.

The reactivity of bromide towards hydroxyl radicals and a resulting reduction of radiolytic H_2O_2 yields was reported already in the 1950s [55, 56]. The properties of bromide as a hydroxyl radical scavenger have since then been used in various applications. As discovered by Matheson et al. [57], the first step of the reaction between hydroxyl radicals and bromide ions is a reversible reaction resulting in the formation of an intermediate species, according to reaction 3.35. Subsequent reactions include reactions 3.36 through 3.38, as well as reactions involving H^+ or other species, depending on the prevailing conditions [57-60].

$$Br^- + \cdot OH \rightleftarrows BrOH \cdot^- \tag{3.35}$$

$$BrOH \cdot^- + Br^- \rightleftarrows Br_2 \cdot^- + OH^- \tag{3.36}$$

$$BrOH \cdot^- \rightleftarrows Br \cdot + OH^- \tag{3.37}$$

$$Br \cdot + Br^- \rightleftarrows Br_2 \cdot^- \tag{3.38}$$

The kinetics of hydroxyl radical scavenging by bromide are approximately 250 times faster compared to the reaction of hydroxyl radicals with hydrogen (reaction 3.34). Furthermore, reactions with reducing species from water radiolysis can result in the reproduction of bromide ions in the solution. This recycling of bromide has been confirmed in radiolysis experiments, where constant bromide concentrations were measured despite their evidential scavenging of hydroxyl radicals [61].

For the case of γ-radiolysis the presence of bromide ions has been shown to give increased radiolysis yields and to interfere with the protective effect of hydrogen on fuel dissolution [62, 63]. However, in radiolysis originating from high LET radiation, such as α-radiation, the scavenging effect of bromide is considered to be negligible due to the limited escape of radicals from the dense radiation spurs [64].

4. Materials and Methods

This chapter presents the materials used in the experimental studies, together with an overview of the analytical methods used for measurements.

4.1. Autoclaves

All radiolysis experiments were performed in stainless-steel autoclaves (Parr) with 450 mL inner volume. Modifications were made to the original design in order to minimize hydrogen leakage. These modifications included changes of valves and connections from NPT to VCR-type connections with Ni gaskets. The autoclaves were sealed with graphite gaskets.

All aqueous solutions were contained in Pyrex beakers or vials inside the autoclaves. For the homogeneous radiolysis study the inner volume of the autoclaves was reduced to 249 mL by the addition of glass beads, as shown in Figure 5, in order to facilitate measurements of oxygen gas in small amounts. For the leaching studies the autoclaves were assembled with stainless-steel dip tubes for water sampling.

Figure 5. Assembled autoclaves (left picture). Inside of autoclave for homogeneous radiolysis experiment, including vial for ^{238}Pu solution and glass beads for volume reduction (right picture).

4.2. ^{238}Pu

For preparation of the high activity plutonium solution for the homogeneous radiolysis experiments, PuO_2 powder was used, with isotopic composition as specified in Table 4. Previous to the preparation from powder, successful oxidations and neutralizations were

achieved using an acidic Pu stock solution originating from the same batch of $^{238}PuO_2$, but with lower specific activity.

Table 4. Original isotopic composition of the $^{238}PuO_2$ powder.

^{238}Pu	^{239}Pu	^{240}Pu	^{241}Pu	^{242}Pu
89.90%	9.182%	0.886%	0.033%	0.008%

4.3. SIMFUEL

The SIMFUEL pellet used for the leaching experiments originated from Atomic Energy Canada Limited (AECL). It consisted of uranium dioxide of natural isotopic composition with additions of Sr, Y, Zr, Mo, Ru, Rh, Pd, Ba, La, Ce and Nd as simulated fission products. Details on the production and characterization of SIMFUEL has been described by Lucuta et al. [65]. The geometrical surface area of the pellet was 339 mm^2.

4.4. MOX pellet

The MOX pellet was supplied by SCK·CEN, Belgium. At the time of experiment the pellet contained approximately 24% plutonium of mixed isotopic composition, together with 1% americium and traces of neptunium from the decay of ^{241}Pu. The original composition is shown in Table 5 as percent by weight of the total oxide mass, together with the composition at the time of the experiment as calculated from decay equations. In order to decrease the total dose the pellet was cut before experiment start. The piece used for leaching was in the form of a half cylinder with 4.43 mm height and a diameter of 8.73 mm, corresponding to a geometrical surface area of 159 mm^2.

Table 5. Composition of the MOX material as wt% of total oxide mass.

	Composition	
	Original	**Feb. 2017**
^{234}U		0.06%
^{235}U	0.19%	0.19%
^{236}U		0.01%
^{238}U	74.81%	74.83%
^{237}Np		0.01%
^{238}Pu	0.58%	0.52%
^{239}Pu	13.72%	13.71%
^{240}Pu	6.46%	6.45%
^{241}Pu	2.51%	1.34%
^{242}Pu	1.73%	1.73%
^{241}Am		1.15%

4.5. Ozonisation

^{238}Pu solutions for the homogeneous radiolysis experiments were oxidized through contact with a gas stream of ozone produced in a corona discharge-type ozone generator (Triogen, LAB2B). Pure oxygen (AGA) was used as input gas, giving a maximum output of 10 g O_3 per hour. In the ozone generator the O_2 gas passes through an electrical field created on the surface of a ceramic dielectric. The splitting of O_2 molecules caused by the electrical field, followed by recombination of the oxygen atoms with other O_2 molecules, results in the formation of O_3.

The output gas from the ozone generator was led through a thin glass tube of a Pasteur pipette into the Pu solution, which was contained in a tall glass vial. The input gas flow was regulated to give a steady stream of bubbles through the solution at an approximate flow rate of 5-10 mL per minute.

4.6. HTTA extraction

In the preparation of ^{238}Pu solutions solvent extraction followed by liquid scintillation counting (LSC) was used as a method for oxidation state determination. The technique of solvent extraction is based on the ability of a ligand to extract certain species from an aqueous phase to an organic phase. HTTA (2-theonyl-trifluoro acetone) is a ligand that can be used to separate plutonium in different oxidation states from each other, depending on the acidity of the aqueous phase [66, 67].

The selective extraction of tetravalent plutonium over plutonium in its other oxidation states was in this case achieved using an aqueous phase of approximately 0.5 M HNO_3. The organic phase was prepared by dissolution of HTTA (99%, Acros Organics) in toluene (puriss, Sigma-Aldrich) to a concentration of 0.25 M. The plutonium sample was added as a spike to the aqueous phase immediately before extraction in order to avoid or minimize oxidation state changes caused by the change in solution conditions. The extractions were performed using equal volumes of each phase, which were contacted in glass vials shaken by hand for 5 minutes. The samples were left to separate by gravity, after which both phases were sampled and measured with respect to Pu activity using liquid scintillation counting (Wallac, 1414 WinSpectral). The distribution ratio of the Pu obtained from the LSC measurement was used as a measure of the oxidation progress in the solution during ozonisation.

4.7. Gas mass spectrometry

All gas analyses were performed using a quadrupole gas mass spectrometer (OmniStar^{TM}, Pfeiffer Vacuum) with an additional motorized gas regulating valve (EVR116, Pfeiffer Vacuum) and external control unit (RVC300, Pfeiffer Vacuum). For ion detection the secondary electron multiplier (SEM) detector was selected in all measurements. The instrument is also equipped with a Faraday cup detector, but the SEM detector is better suited for low concentration measurements because it gives a larger amplification of the signal. The instrument was operated at a set inlet pressure of $3 \cdot 10^{-6}$ mbar.

For all radiolysis experiments the sampling system was constructed using pre-welded CT tubes (Swagelok) and VCR connections with Ni gaskets. An external pumping station (TSH 071 E, Pfeiffer Vacuum) was connected as part of the sampling system for evacuation.

Data evaluation of the $^{18}O_2$ measurements described in Paper I was based on the isotopic content in air. All other data evaluation was based on measurements of calibration gases, as well as the background gases used for pressurization of the autoclaves in the different experiments. A compilation of the gases used for analysis is shown in Table 6.

Table 6. Gases used for calibrations and background measurements for mass spectrometric analysis in the radiolysis experiments.

Gas	Specification	Supplier
H_2	99.9%	AGA
50 ppm O_2 in H_2	Oxygen N45 46.6 ± 0.93 mol-ppm Hydrogen N30 rest	Air Liquide
500 ppm O_2 in H_2	Oxygen N45 464.5 ± 9.3 mol-ppm Hydrogen N30 rest	Air Liquide
Ar	Instrument Argon 5.0, 100%	AGA
Ar	Ar ≥ 99.999% $H_2O \leq 3$ ppm, $O_2 \leq 2$ ppm, $C_nH_m \leq 0.5$ ppm	Air Liquide
1000 ppm O_2 in Ar	Oxygen 974 ± 2 mol-ppm	AGA
D_2 with 30 ppm CO_2	Carbon dioxide 28.0 mol-ppm measurement uncertainty ± 2%	Linde Gas

4.8. H_2O_2 measurement

Concentrations of hydrogen peroxide were measured spectrophotometrically (Shimadzu, UV-1800) at 350 nm using the tri-iodide method as described by Ghormley et al. [55, 68, 69]. The method is based on oxidation of iodide by H_2O_2 followed by formation of tri-iodide according to reactions 4.1 and 4.2. The oxidation reaction is carried out with an excess of iodide in neutral or slightly acidic conditions in the presence of a molybdate catalyst.

$$2I^- + H_2O_2 \rightarrow I_2 + 2OH^- \quad (4.1)$$

$$I_2 + I^- \rightarrow I_3^- \quad (4.2)$$

The instrument was calibrated in connection with each measurement using a set of calibration solutions, in the range of 0.01-0.1 mM, prepared by dilution of H_2O_2 (30 wt% in H_2O) with MilliQ water (18.2 MΩ). For sample preparations the following solutions were used:

- 1 M potassium iodide (KI ≥99.5%, Sigma-Aldrich, dissolved in MilliQ water)
- 3% ammonium molybdate tetrahydrate (≥99.0%, Sigma-Aldrich, dissolved in MilliQ water)
- acetate buffer solution (pH 4.65, Sigma-Aldrich)
- H_2O_2 calibration or sample solution

All samples were prepared by mixing 100 µL KI solution and 100 µL ammonium molybdate tetrahydrate in acetate buffer with 2 mL of the sample or calibration solution in a 1 cm cuvette. The time between sample preparation and measurement was 5 minutes. Depending on the

expected H_2O_2 concentration, the samples were in some cases diluted with MilliQ water in connection with the sample preparation.

4.9. HDO measurement

The reason for using deuterium instead of ordinary hydrogen in the leaching experiments was to facilitate the detection of any water possibly produced in the reaction between hydroxyl radicals and dissolved hydrogen. With deuterium, the product of this reaction (4.3) would be HDO, which could be quantified by isotopic analysis.

$$D_2 + 2OH \cdot \rightarrow 2HDO \tag{4.3}$$

Measurements of deuterium content in the leachates were performed at the UC Davis Stable Isotope Facility, CA. The instrument used was a Liquid Water Isotope Analyzer (LWIA, Los Gatos Research, Inc.). With this method, based on laser absorption in water molecules, absolute abundances of HDO and H_2O are quantified through measurement of the absorbances at their respective wavelengths. The method can also be used for quantification of $H_2{}^{18}O$ [70].

The results are presented as per mil deuterium according to equation 4.4, where *D/H* is the atomic ratio of deuterium to hydrogen and the index *SMOW* refers to Standard Mean Ocean Water with isotopic ratio $155.76 \cdot 10^{-6}$ [71].

$$\delta D = \frac{\left(\frac{D}{H}\right)_{sample} - \left(\frac{D}{H}\right)_{SMOW}}{\left(\frac{D}{H}\right)_{SMOW}} \tag{4.4}$$

4.10. ICP-MS

Inductively coupled plasma mass spectrometry (ICP-MS) (Thermo Scientific iCAP Q) was used for measurements of dissolved actinides in the leaching studies. For SIMFUEL leaching the U concentration was determined by ICP-MS measurement at mass 238, from which the total concentration could be calculated based on the ^{238}U natural abundance. For MOX leaching the results from ICP-MS measurements at masses 234 through 242 were combined with results from radiometric measurements in order to determine the total concentrations of U, Pu and Am, as explained further in section 4.13.

All samples were prepared by dilution with 0.5 M HNO_3 (65% suprapur, Merck). Calibration solutions were prepared by dilution of a ^{238}U standard to concentrations in the range 0-50 ppb. Th was used as an internal standard in the samples, as well as in the calibration solutions.

4.11. α-spectrometry

In the MOX leaching experiments α-spectrometric measurements (Ortec, Alpha Duo, Octête TM PC) of the leachate samples were performed and the data was used in combination with ICP-MS and HPGe data for determination of actinide concentrations. Some of the nuclides present in MOX fuel are indistinguishable with respect to α-energies, which is why the combination of different measurement methods was necessary. The measurements showed one peak at 5.2 MeV, representing the sum of ^{239}Pu and ^{240}Pu, and one peak at 5.5 MeV, representing ^{238}Pu and ^{241}Am.

A standard sample was prepared from a ^{241}Am stock solution and used for determination of the detector efficiency. All samples were prepared by mixing 10 µL of the leachate sample with 100 µL coating solution (Z-100) on a planchet, followed by 10 minutes drying under an IR lamp. Before measurement the planchet was heated using a gas burner in order to remove any residual acetone from the coating solution.

4.12. HPGe

γ-spectrometric measurements of ^{241}Am at 59.6 keV were performed using a high purity germanium (HPGe) detector (coaxial Ortec GEM-C5060 coupled with the digital spectrum analyzer Ortec DSPEC50). The efficiency was determined based on measurements of ^{241}Am standard solutions with geometry equal to the samples.

4.13. Calculation of actinide concentrations

Due to overlaps, both of masses and α-energies for some of the nuclides present in the MOX fuel, a combination of mass spectrometric and radiometric methods was used. The ^{238}Pu activity was determined by subtraction of the ^{241}Am activity as obtained in the γ-measurements from the activity measured at the 5.5 MeV α-peak. With known ^{238}Pu and ^{241}Am activities, the concentrations of ^{238}U and ^{241}Pu could be calculated from the results of the mass spectrometric measurements. The activities measured at the 5.2 MeV α-peak were compared with the mass spectrometric data for verification of the measured efficiency.

5. Experimental

The experimental work in this thesis is based on three different sets of experiments; homogeneous radiolysis, leaching of SIMFUEL and leaching of un-irradiated MOX fuel. All experiments were performed in autoclaves, as described in Chapter 4.1, under a hydrogen or argon atmosphere. The work on plutonium oxidation and stabilization was part of the preparations for the homogeneous radiolysis studies, as these required a high activity α-emitter in neutral solution. This chapter provides a description of the experimental details for each study.

5.1. Preparation of ^{238}Pu solution

Neutral ^{238}Pu solutions were prepared, starting with dissolution of PuO_2 powder or an acidic Pu stock solution. The plutonium was oxidized from Pu(IV) to Pu(VI) and complexed with carbonate in order to increase the solubility and stabilize the plutonium in solution during neutralization. The different steps of the solution preparation are described in more detail in the following sections.

5.1.1. Dissolution of PuO_2

PuO_2 powder was dissolved in concentrated HNO_3, yielding a 3 GBq/mL solution as measured by liquid scintillation counting. Complete dissolution was achieved within a few hours with no heating applied. The dissolution was performed in a nitrogen atmosphere glove box. As shown in Figure 6, the solution had a dark green colour, typical for tetravalent plutonium in nitric acid.

5.1.2. Oxidation of Pu(IV)

Oxidation of the tetravalent plutonium was achieved by addition of ozone through the solution as described in Chapter 4.5. Before preparation of the stock solution an ozonisation test was carried out using a more dilute plutonium solution. The rate of oxidation was investigated, as well as the stability of the hexavalent Pu in the absence of ozone. The change in oxidation state was verified by HTTA extraction of 10 µL samples at regular time intervals, and the sampling was continued until sufficient oxidation was achieved, i.e. until the distribution ratio between the plutonium in the organic phase and the aqueous phase was sufficiently low. For the case of the stock solution, some dilution proved necessary in order to reach complete oxidation of the plutonium.

5.1.3. Carbonate complexation and neutralisation

For simultaneous carbonate complexation of the hexavalent plutonium and neutralization of the acidic solution, a 7 M NaOH solution with 1 M $NaHCO_3$ was introduced by dropwise addition during continued ozonisation. During the last stage of neutralization the ozone bubbling was interrupted to facilitate continuous pH measurement. A dilution of the NaOH solution was used for pH adjustment. Figure 6 (right picture) shows a stabilized and neutralized solution.

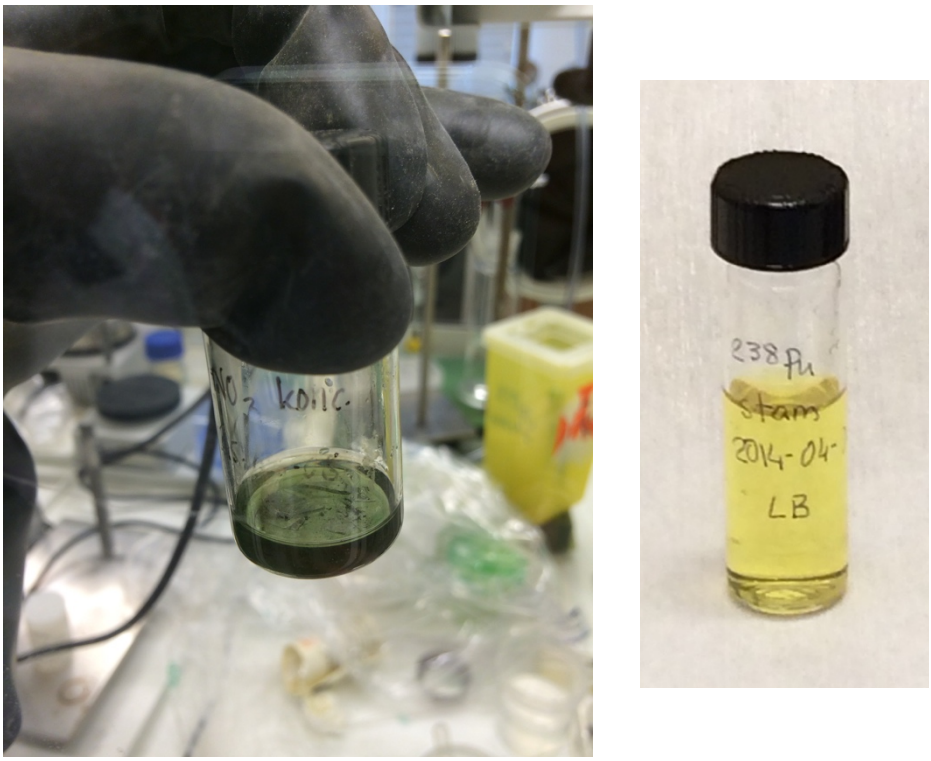

Figure 6. $^{238}PuO_2$ dissolved in concentrated HNO_3 (left picture). ^{238}Pu solution after oxidation, carbonate complexation and neutralization (right picture).

5.2. Homogeneous radiolysis

In the homogeneous radiolysis experiments the ^{238}Pu solution was placed in open glass vials inside the autoclaves. The total activity in each autoclave was approximately 570 MBq. For the H_2 experiments aliquots of the same solution were used in parallel experiments, one of which was spiked with 7.5 µL 0.4 M NaBr, for a total Br^- concentration of 1 mM. An equivalent experiment was also performed under Ar, in order to investigate the hydrogen effect.

After initial pressurization with H_2 or Ar, each autoclave was sealed by daily re-tightening of the bolts, which results in successive deformation of the graphite gasket. Once the sealing was complete the autoclave was pressurized with new gas and the experiment was started. The final pressurization was preceded by repeated filling and evacuation for 10 consecutive cycles, in which the last two included evacuation to the millibar range using the external pumping system. The H_2 or Ar pressure at the start of each experiment was 1 MPa.

On each sampling occasion the autoclave was connected to the gas mass spectrometer via the sampling system described in section 4.7, and the gas phase was analysed with respect to radiolytically produced O_2. When the autoclave was opened at the end of experiment the solution was sampled and analysed with respect to H_2O_2 concentration.

5.3. SIMFUEL leaching

In order to remove the oxidized layer the SIMFUEL pellet was subjected to pre-leaching in 10 mM $NaHCO_3$ solutions before the start of each experiment series. The pre-leaching was performed under argon purging of the solution in cycles of 30 minutes, with exchange of solutions between each cycle. The solutions were sampled and measured with respect to

uranium concentration in order to determine when sufficiently low levels had been reached. After pre-leaching the pellet was rinsed with MilliQ water and immediately transferred to the autoclave, together with leaching solution and H_2O_2.

The leaching was conducted in 10 mM NaCl and 2 mM $NaHCO_3$, or in 10 mM $NaHCO_3$, with 10 bar initial D_2 pressure. Leachate samples were taken at regular time intervals, and the experiments were continued until the H_2O_2 concentrations in the leachate samples were below detection limit. Apart from H_2O_2, the leachate samples were also analysed with respect to U and HDO concentrations. Qualitative analysis of the gas phase was performed after leaching.

5.4. MOX leaching

For the case of MOX leaching, removal of the oxidized layer was achieved by annealing in 5% H_2 in N_2 at 1200ºC for 5 hours with 5ºC/min heating and cooling rate. The annealing was performed in a furnace (1000-2560-FP20 High Temperature Graphite Furnace, Thermal Technology) inside a nitrogen atmosphere glove box. After heat treatment, the pellet was immediately transferred from the glove box to the autoclave containing leaching solution purged with deuterium or argon gas.

Two leaching experiments were performed; one under Ar and one under D_2 atmosphere. The same piece of MOX was used in each of the two experiments. The leachate was sampled and analysed with respect to U, Pu and Am concentration, as well as H_2O_2 and HDO concentrations.

6. Results and Discussion

In this chapter the results of the radiolysis studies are presented and discussed with the intention of providing an overview of result interpretations and possible implications with respect to long-term fuel storage. For further elaborations on the results of each separate experiment the reader is referred to the material presented in Papers II through IV. The following sections also discuss some technical issues encountered during the preparations for, and execution of, the radiolysis experiments.

6.1. Plutonium oxidation and reduction in solution

The results of the plutonium oxidation tests by ozonisation are shown in Figure 7 as percent Pu extracted by HTTA. In this case complete oxidation was achieved after approximately 3 hours of ozone bubbling through the solution. Oxidation of the high activity solutions proved to be significantly slower, however, and dilution of the solution was required in some cases before sufficient oxidation could be achieved.

As HTTA selectively extracts Pu(IV) under the prevalent conditions, the results reflect the amount of Pu(IV) present in solution at each time of sampling. The remaining plutonium is assumed to be present as Pu(VI), based on the high tendency for Pu(V) disproportionation, in combination with the fact that oxidation states VII and higher can only be reached in alkaline conditions, if at all.

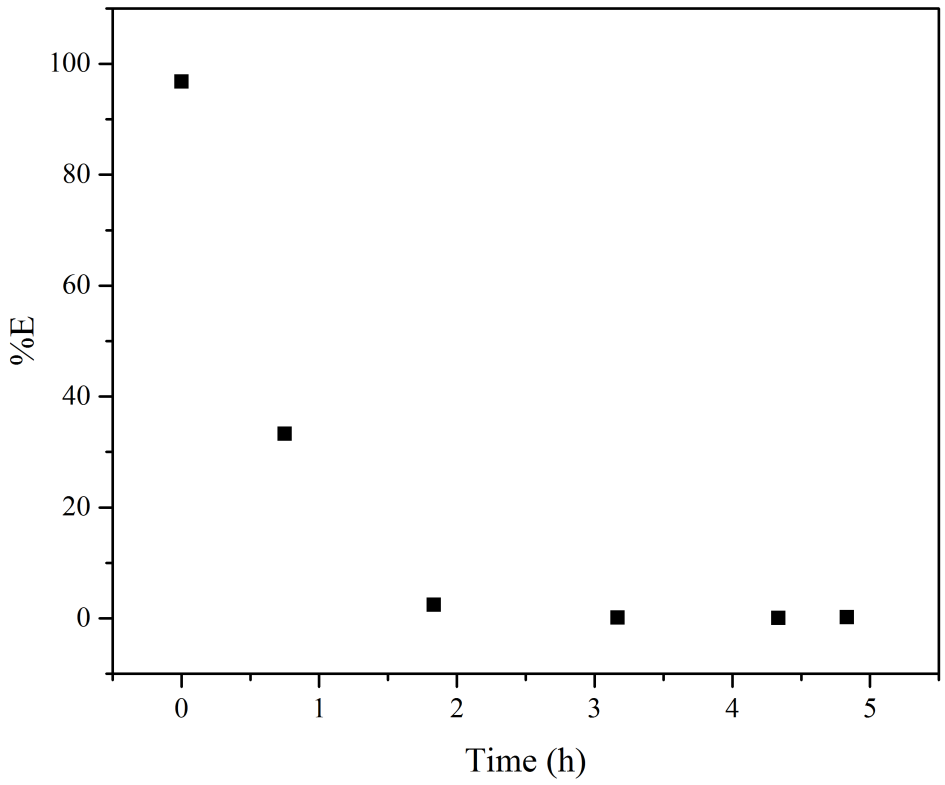

Figure 7. Pu(IV) extraction by HTTA during ozonisation of the test solution

In order to investigate the possible reduction of the oxidized Pu in the absence of ozone the sampling of the test solution was continued after the ozonisation was stopped. The results of the extractions showed a continuous increase of Pu(IV), although at a significantly slower rate compared with the oxidation, as shown in Figure 8. The comparatively slower reduction facilitated ozonisation in intervals, which was necessary for oxidation of the more concentrated solutions for which the total ozonisation time was considerably longer.

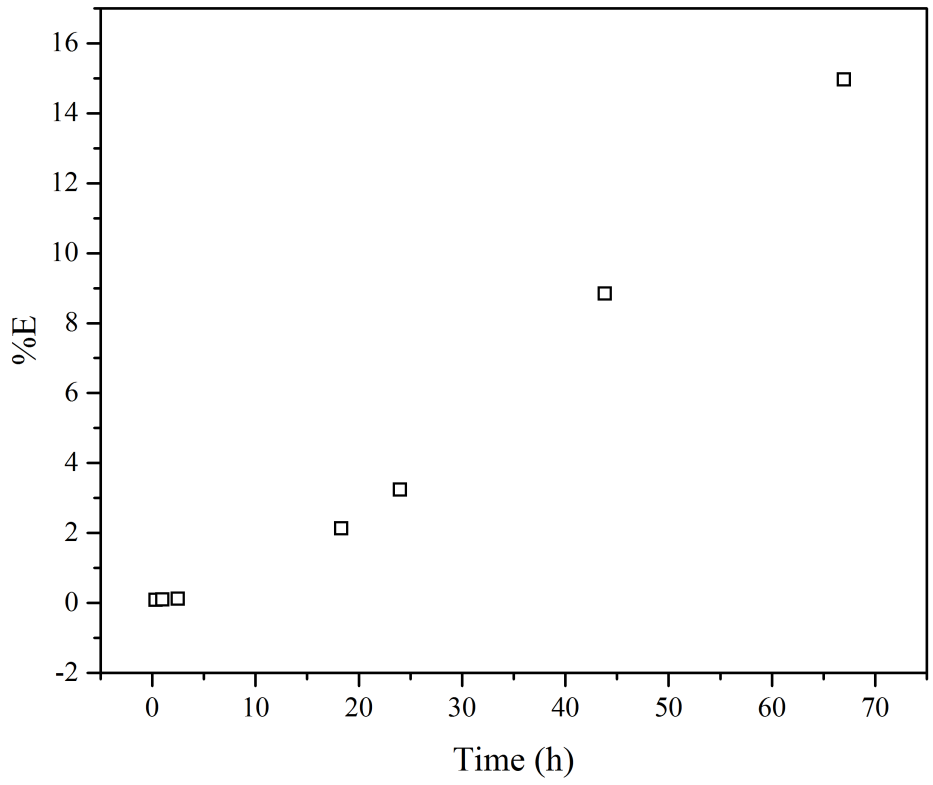

Figure 8. Pu(IV) extraction by HTTA after ozonisation of the test solution.

6.2. Oxygen measurements

Mass spectrometric measurements of ppm range concentrations of oxygen gas are inherently complicated by the presence of oxygen in air. The experiments presented in this thesis are conducted in autoclaves stored in an air atmosphere, and the gas measurements are performed by connection of the autoclaves to the gas mass spectrometer via a sampling system in which the gas is expanded in order to reach a pressure suitable for measurement. The quality of such measurements is entirely dependent on the minimization of influence from ambient air in the autoclaves and in the sampling system. Alterations between vacuum and overpressure in the system also imposes special requirements on the equipment with respect to leakage prevention, as does the use of hydrogen in many of the experiments.

Modifications to the original design of the autoclaves included exchange of all connections, valves and manometers from standard NPT to Swagelok VCR connections sealed with Ni gaskets. This type of connection is better suited for repeated assemblies as the sealing is based

on deformation of an exchangeable metal gasket. The sampling system was constructed using pre-welded flexible convoluted metal tubes, also with VCR connections.

In-leakage of air can be monitored by observation of the nitrogen signal (or other suitable components of air such as argon) during measurements. However, if the contribution to the oxygen signal from ambient air is to be quantified based on the presence of other air components, a couple of issues need to be taken into account. First of all, different ionization probabilities and pumping efficiencies apply to different gases, which means that the signal-to concentration relation varies depending on type of gas. Hence, the composition of air does not necessarily correspond to the relation between measured signals. In addition, the sensitivity of the SEM detector is mass specific, which further enhances this effect. Finally, gas diffusion is driven by differences in partial pressure rather than total pressure, which means that the air that leaks in does not necessarily have the same composition as the ambient air.

Differences in ionization probabilities also result in the fact that for any given molecule the sensitivity of the instrument can differ depending on the type of carrier gas. If for example the carrier gas has a high ionization probability, resulting in a relatively high ion density in the formation space, the overall sensitivity will be lowered. Calibration gases with different concentrations of oxygen in hydrogen or argon background were therefore used for quantitative measurements of oxygen in the radiolysis experiments. Measurements showed that the calibration of oxygen with hydrogen as the carrier gas was not valid for oxygen measurements in a deuterium background, which is why the measurements from the deuterium experiments were only given a qualitative evaluation.

For oxygen measurements in a given carrier gas a linear relation between signal and concentration can be expected. However, during measurements spanning very wide concentration ranges, such as the oxygen measurements described in Paper I where different isotopes are analysed simultaneously, effects of non-linearity should be taken into account. The oxygen production in this type of experiment is traced by the use of ^{18}O-enriched water and can therefore be measured at masses 34 and 36 for the presence of $^{16}O^{18}O$ and $^{18}O_2$, respectively. A net consumption of oxygen is simultaneously measured at mass 32, at percent level. Since the carrier gas in this case was air, effects of non-linearity could be corrected for by using two different calibrations based on oxygen isotopic content in the ambient air. For the ppm range, the calibration was based on natural abundance of $^{16}O^{18}O$, whereas the calibration for percent levels was based on $^{16}O_2$. A more detailed description of the calibration procedure and data evaluation is given in the supplementary material accompanying Paper I.

6.3. Bromide effect during α-radiolysis

The objective of the bromide study was to investigate whether or not the presence of bromide in groundwater would influence the yields of oxidants produced during α-radiolysis under a hydrogen atmosphere. Two experimental series were run in parallel using aliquots of the same ^{238}Pu solution, one of which was spiked with Br^- yielding a total concentration of 1 mM.

The oxygen concentration measured in the gas phase is shown in Figure 9, together with the pressure readings from the autoclaves. The stepwise pressure drop is the result of gas sampling and has to be taken into account in the data evaluation.

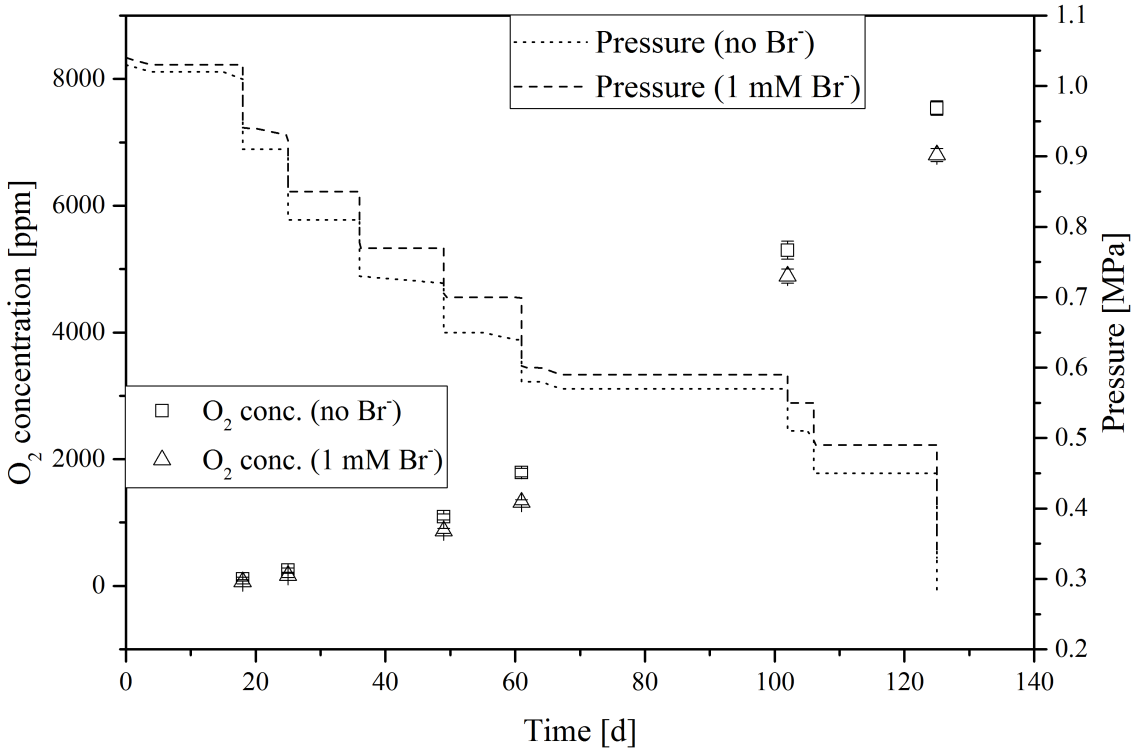

Figure 9. O_2 concentrations at each time of measurement (left scale), together with pressure logs for the two autoclaves (right scale).

In Figure 10, the data is presented as total amount of oxygen produced in each autoclave as a function of α-dose to the solution. The uncertainties shown in the figures were calculated based on standard deviations of the oxygen measurements.

Comparison of the oxygen production in the two series shows that the addition of bromide had no significant effect on the oxygen radiolytic yield. Since O_2 originates from H_2O_2 decomposition these results indicate that there is no interference of Br^- with radiolytic H_2O_2 production. This conclusion is supported by the results of the spectrophotometric measurements of H_2O_2 content in each solution at the end of the experiment, as shown in Table 7.

Table 7. H_2O_2 concentration in the ^{238}Pu solutions at the end of the homogeneous radiolysis experiment under H_2 atmosphere. Uncertainties are based on volumetric measurements during sample dilutions and correspond to 2σ.

	H_2O_2 concentration
^{238}Pu solution without Br^-	1.1 ± 0.1 mM
^{238}Pu solution with 1 mM Br^-	0.9 ± 0.1 mM

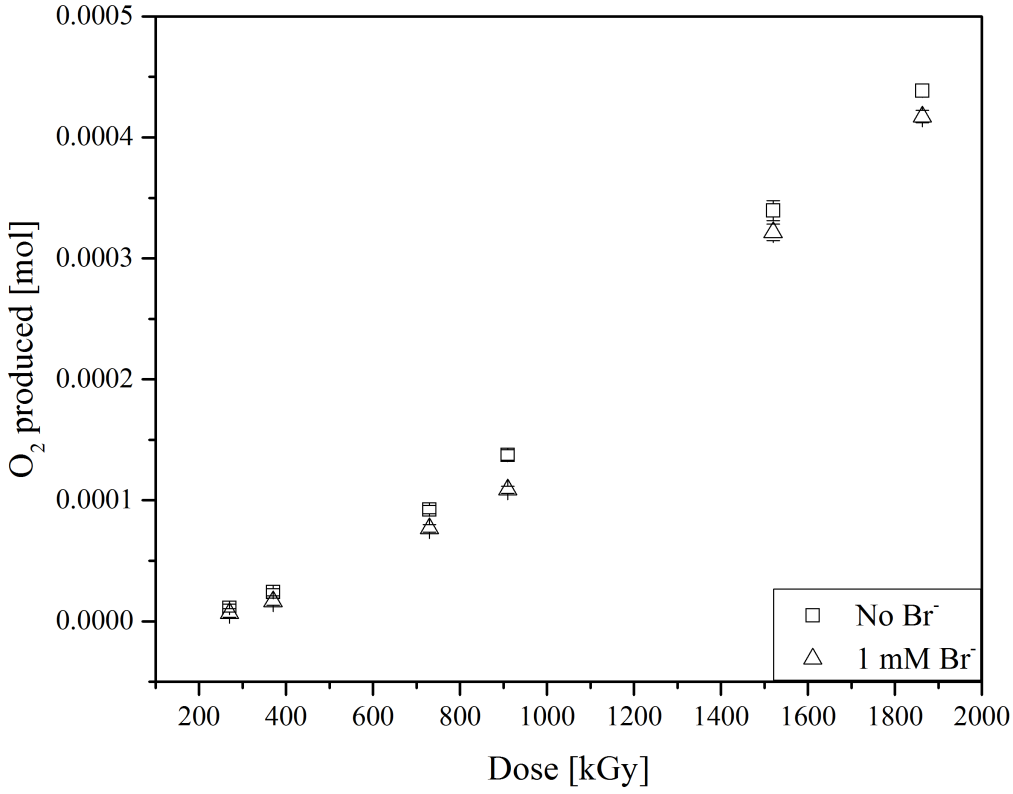

Figure 10. Total production of O_2 as function of α-dose to the water during the homogeneous radiolysis experiment under H_2 atmosphere. The error bars represent measurement uncertainties corresponding to 2σ.

It should be noted in this context that spectrophotometric measurements of H_2O_2 in highly active solutions present some difficulties due to continued radiolysis resulting in a continuous increase of H_2O_2 in the sample during and after its preparation. The uncertainties given in Table 7 may thus be underestimated, since the values only reflect the standard deviation based on volumetric measurements during the sample preparations. The results should however represent an accurate comparison of the two samples.

The absence of a bromide effect during α-radiolysis is consistent with the reasoning of Crumière et al. [64] based on the low radical yields from high LET radiation. In the context of fuel corrosion the result may seem contradictory to the conclusions drawn by Metz et al. [63] based on an increased Sr release during leaching of spent fuel in the presence of bromide. However, as highlighted in a later publication [72], the release rate of Sr may not be an adequate indicator for fuel matrix dissolution, and the higher Sr concentrations could possibly be an effect of a shorter wash cycle in the bromide experiment compared with the reference case [48, 73].

6.4. Homogeneous radiolysis

In order to investigate the hydrogen effect in the bulk solution during α-radiolysis one series of the homogeneous radiolysis experiment was conducted under an Ar atmosphere, the results of which are presented in Figure 11, together with the results of the H_2 series without Br^- addition. In comparison with these results, it is clear that the O_2 production lies within the same range regardless of atmosphere. This leads to the conclusion that there is no suppression of H_2O_2

production, despite the presence of dissolved H_2 in the water. These results are in agreement with a previous study of homogeneous α-radiolysis in acidic ^{238}Pu solutions [74].

The lack of hydrogen effect in homogeneous α-radiolysis, in combination with the hydrogen effect seen in leaching of α-doped fuel [11, 42, 50], confirms the role of surface processes as discussed by Cui et al. [75].

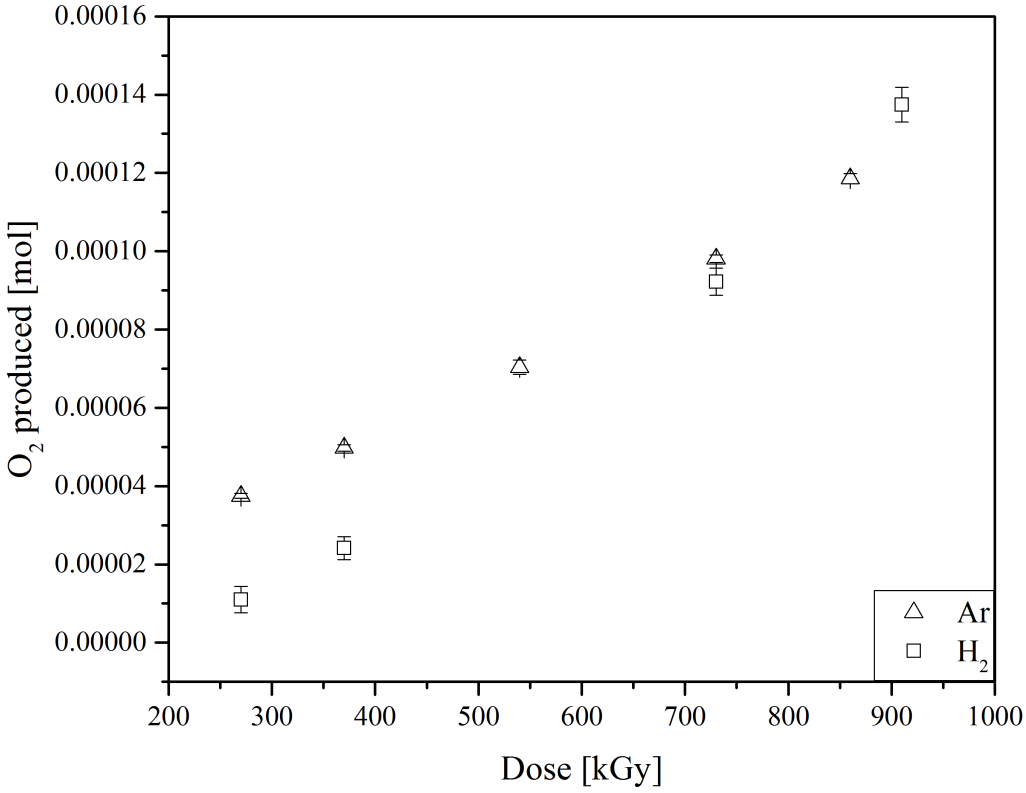

Figure 11. Total production of O_2 as a function of α-dose to the water during the homogeneous radiolysis experiment under H_2 and Ar atmosphere. The error bars represent measurement uncertainties corresponding to 2σ.

As mentioned previously, studies of homogeneous α-radiolysis, as opposed to using external radiation sources, can be advantageous with respect to dose distribution. It should however be noted that the use of highly active solutions in this type of experiment means that the accuracy in dose determination is limited by the uncertainties in volumetric measurement, which for small volumes can be relatively large. This issue must be taken into account when comparing the results of the H_2 and Ar series, since different solutions were used. For the bromide study however, aliquots of the same solution were used in parallel experiments, which means that although there may be a non-negligible uncertainty in total dose, the comparison between the two series should be accurate.

6.5. H_2O_2 decomposition

Radiolytically produced hydrogen peroxide in a deep repository can be consumed in oxidation of the fuel matrix, by catalytic decomposition on the fuel surface, or by decomposition in the bulk solution. The hydroxyl radicals formed in the first step of the decomposition react further to form water and oxygen, unless scavenged by hydrogen, in which case the resulting product is water only. The fate of hydrogen peroxide could thus hypothetically be described by any of the following three paths:

i) Oxidation of U(IV) resulting in dissolved U
ii) Decomposition of H_2O_2 resulting in formation of H_2O and O_2
iii) Decomposition of H_2O_2 followed by reaction of ·OH with H_2 resulting in formation of water

In the view of preventing fuel dissolution, options ii) and iii) are both beneficial, since O_2 is a considerably less reactive oxidant in comparison to H_2O_2. Nevertheless, for further insight into the hydrogen effect complete determination of the fate of H_2O_2 under these conditions is desirable.

In the SIMFUEL experiments the consumption of added H_2O_2 and the dissolution of U were monitored during leaching of SIMFUEL under a deuterium atmosphere. Figure 12 shows the H_2O_2 consumption during three different leaching series, together with the H_2O_2 consumption without the presence of the pellet. It is clear that the H_2O_2 decomposition is enhanced by the presence of the pellet surface, although a significant decrease is noted also for the reference case.

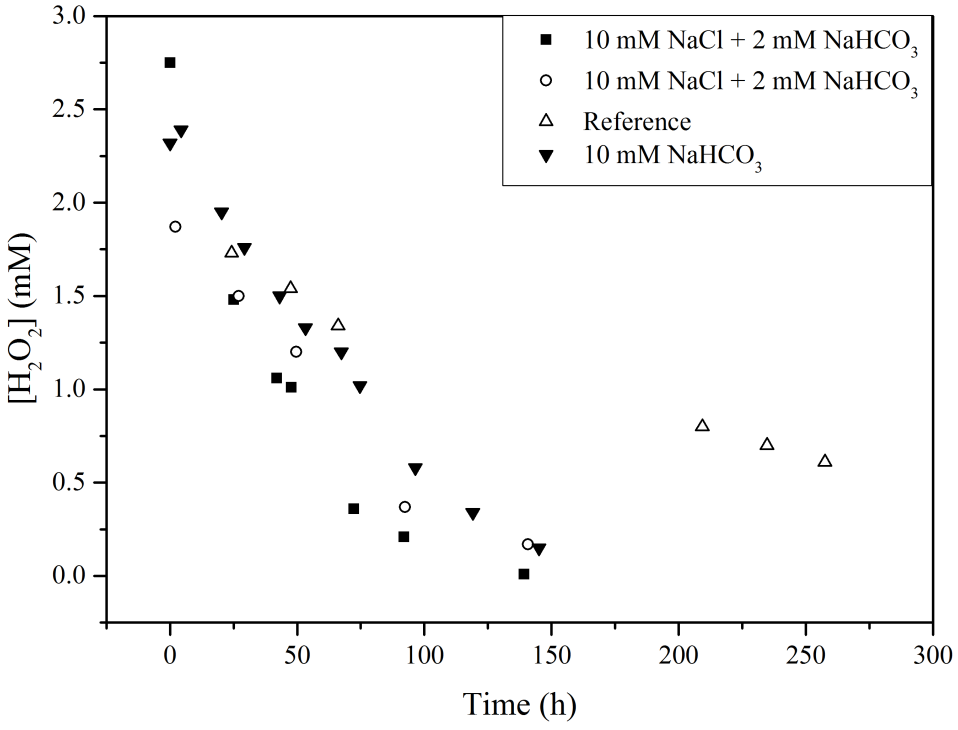

Figure 12. Concentrations of H_2O_2 in the leachate solutions at each time of sampling. The reference case represents the degradation of H_2O_2 in the absence of the SIMFUEL pellet.

Figure 13 shows the uranium concentration in the leachates as measured by ICP-MS. As explained in section 3.4, the higher carbonate concentration causes a more rapid release of the oxidized uranium.

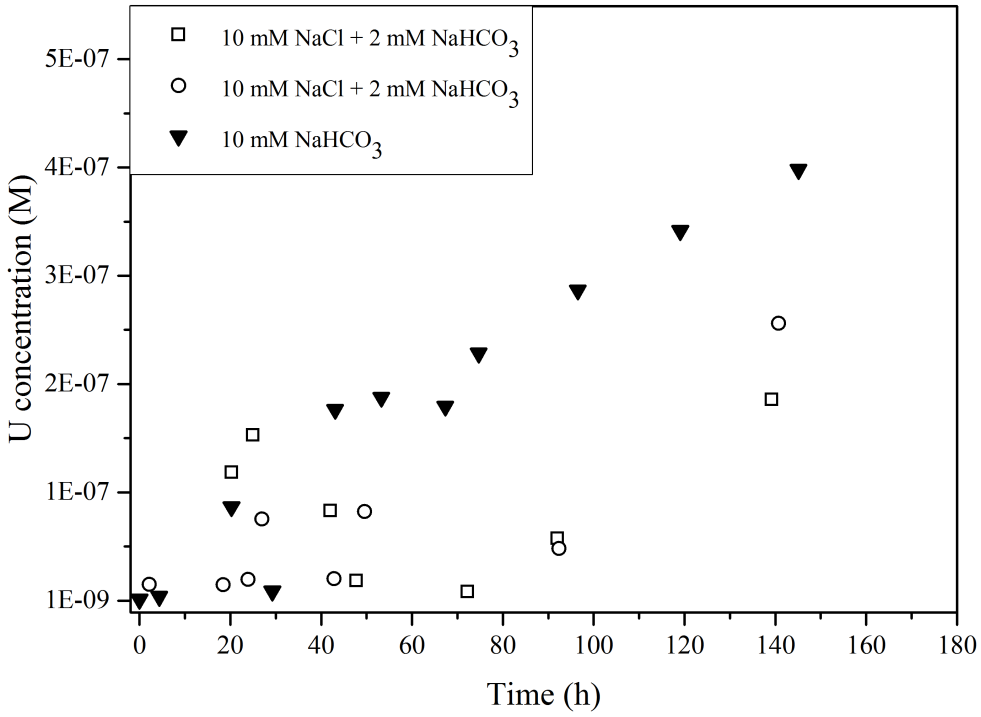

Figure 13. Concentrations of U in the different leachates as functions of time.

A comparison between the amount of H_2O_2 consumed in the autoclave and the total amount of dissolved U is shown in Figure 14, for the case of leaching in 10 mM $NaHCO_3$. The trends are very similar, although the amounts differ by orders or magnitude. Calculations based on this measurement series shows that the amount of oxidized U released in solution corresponds to only 0.02% of the consumed H_2O_2. Consequently, 99.98% of the H_2O_2 consumption must be due to H_2O_2 decomposition according to options ii) or iii).

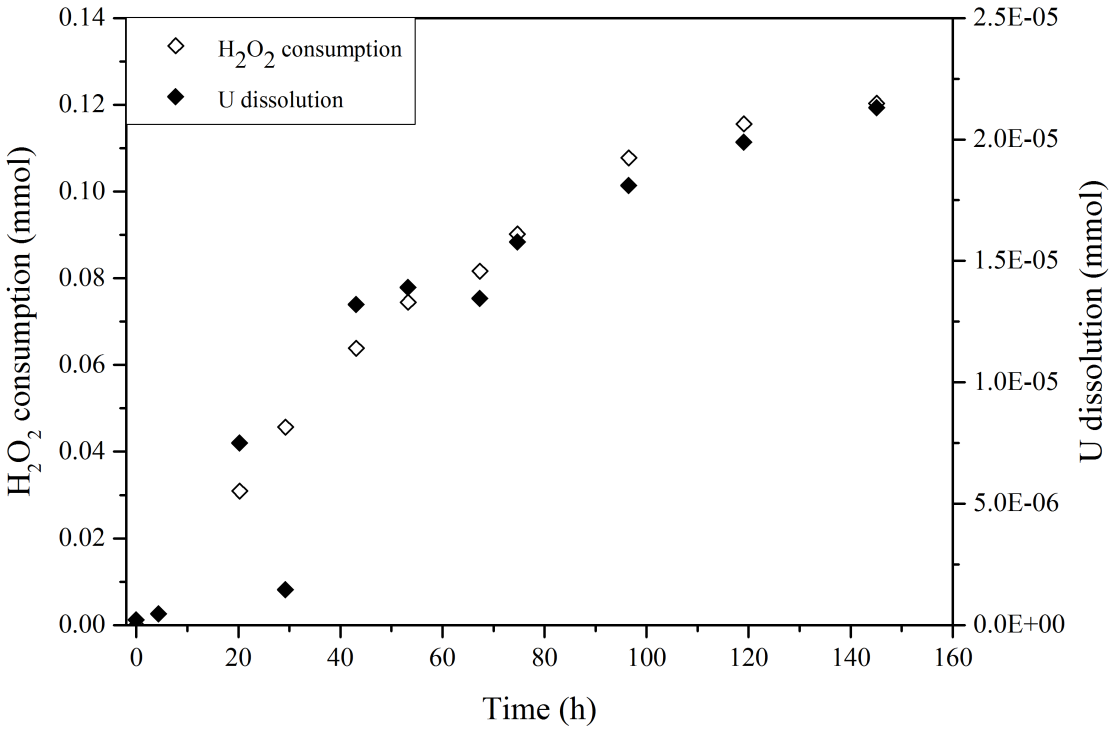

Figure 14. Consumption of H_2O_2 (left scale) in the 10 mM $NaHCO_3$ leachate together with the total U dissolution (right scale).

Possible formation of water according to option iii) was investigated by isotopic analysis of the leachate samples. The formation of HDO as determined in the isotopic analysis is shown in Figure 15 for two of the leachate series, as well as the reference case in which the pellet was omitted.

The results clearly confirm that HDO is formed in the leachate solutions. However, in order to use this result only as proof of the reaction between hydroxyl radicals from H_2O_2 decomposition and dissolved hydrogen (reaction 4.3), all other possible sources of HDO must be ruled out. The experimental setup of the reference series was identical to that of the leaching experiments with the exception of the presence of the fuel surface in each leaching. In this way any contributions to the HDO formation from normal isotopic exchange or H_2O_2 decomposition on other surfaces are accounted for. Nevertheless, this does not provide sufficient evidence of the surface reaction suggested, since the acceleration of isotopic exchange by the presence of the fuel surface cannot be excluded.

In the isotopic exchange between deuterium and water HD is formed in addition to HDO, according to reaction 6.1. Quantification of HD in the gas phase would thus yield the corresponding amount of HDO.

$$D_2 + H_2O \rightarrow HD + HDO \tag{6.1}$$

Unfortunately, mass spectrometric measurements of small amounts of HD gas in a deuterium carrier gas are problematic due to the closeness of the sample peak to the background peak. Scan measurements of the pure D_2 gas showed that the contribution from the background gas at mass 3 was high enough to obstruct HD measurements for concentrations lower than percent level.

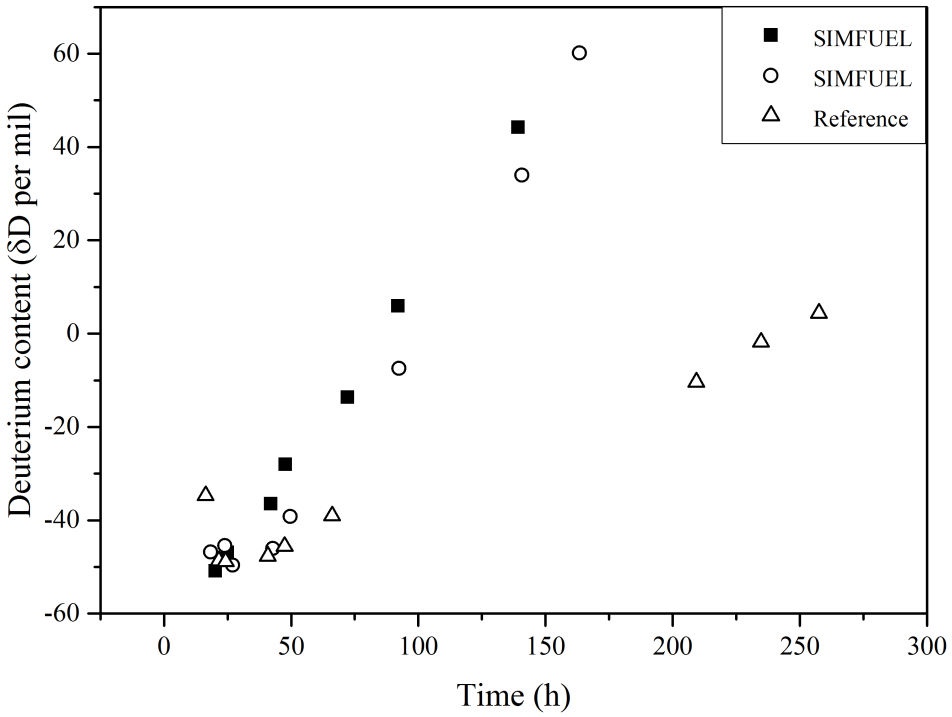

Figure 15. Fraction of deuterium in the water samples from SIMFUEL leaching experiments. The production of HDO in the absence of the SIMFUEL pellet is represented by the reference case. The isotopic content is presented as per mil deuterium with respect to SMOW according to equation 4.4.

Qualitative measurements of oxygen in the gas phase indicated that at least some of the H_2O_2 decomposition proceeded according to route ii). The possibility thus exists that there is no occurrence of the surface reaction suggested in route iii) and that the HDO formation is entirely due to isotopic exchange. However, as explained below, the results of the MOX leaching experiments show that the contribution from route ii) is negligible, thus supporting the hypothesis of a surface reaction as suggested.

The concentrations of U and Pu in solution during the leaching of the MOX piece in the presence of deuterium are shown in Figure 16. The results clearly indicate that there is no oxidative dissolution during the first 30 days of leaching. Furthermore, analysis of the gas phase shows no measurable oxygen production. Hence, options i) and ii) can be dismissed. Finally, isotopic analysis of the water confirms the production of HDO, as shown in Figure 17.

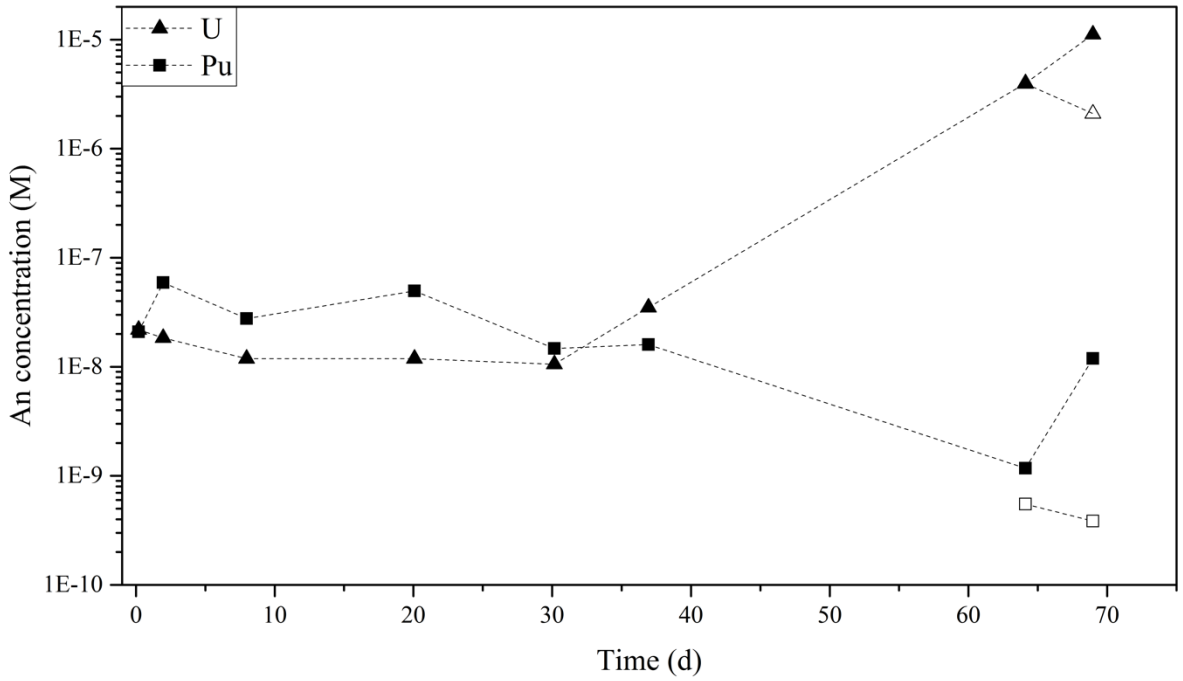

Figure 16. Concentrations of U and Pu in the water during leaching of MOX in the presence of dissolved deuterium. The open symbols at 64 and 69 days represent centrifuged samples.

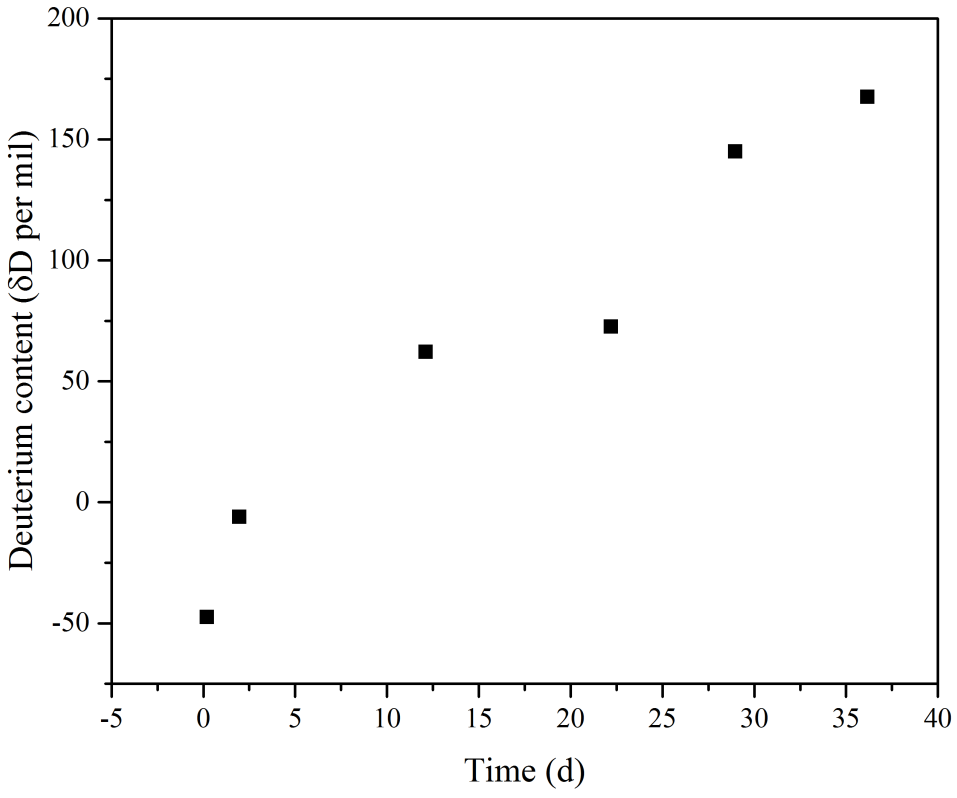

Figure 17. Fraction of deuterium in the water samples from MOX leaching under a D_2 atmosphere. The isotopic content is presented as per mil deuterium with respect to SMOW according to equation 4.4.

6.6. H_2 effect at high α-dose

The MOX fuel used in the leaching experiments had a specific α-activity of 4.96 GBq/g, comparable to the Pu rich agglomerates in irradiated MOX fuel. The results of the leaching experiments under a D_2 atmosphere (Figure 16) clearly showed that during the first 30 days the fuel was completely protected from oxidative dissolution. As a result of leachate sampling there was a gradual pressure decrease over this time period. The autoclave was then subjected to larger pressure drops due to gas sampling during days 42 and 51, after which the uranium dissolution increased significantly. The autoclave pressure at each leachate sampling is presented in Table 8, together with corresponding amounts of dissolved D_2 in the leachate calculated using Henry's law with the constant $7.9 \cdot 10^{-6}$ mol/(m^3Pa) [76]. Based on these results, dissolved hydrogen at concentrations of 6.4 mM and above appears to be sufficient for complete suppression of oxidative dissolution of the MOX. This hydrogen concentration is well below that expected in a geological repository due to canister iron corrosion [77, 78].

Table 8. Autoclave pressure on each leachate sampling occasion in the D_2 experiment, together with the corresponding amount of dissolved deuterium in the water. Calculations based on Henry's law constant for D_2 in water [76].

Leachate sample no.	Pressure in autoclave	Dissolved D_2
1	1.00 MPa	7.9 mM
2	0.96 MPa	7.6 mM
3	0.90 MPa	7.1 mM
4	0.85 MPa	6.7 mM
5	0.81 MPa	6.4 mM
6	0.77 MPa	6.1 mM
7	0.57 MPa	4.5 mM
8	0.55 MPa	4.3 mM

Leaching of MOX was also conducted under an Ar atmosphere for comparison with the D_2 experiment. Although significantly higher U concentrations were measured in this case, the dissolution progress was slower than anticipated based on the high dose rate. However, high Pu contents have been shown to give increased stability towards dissolution, which may provide an explanation for the somewhat unexpected result.

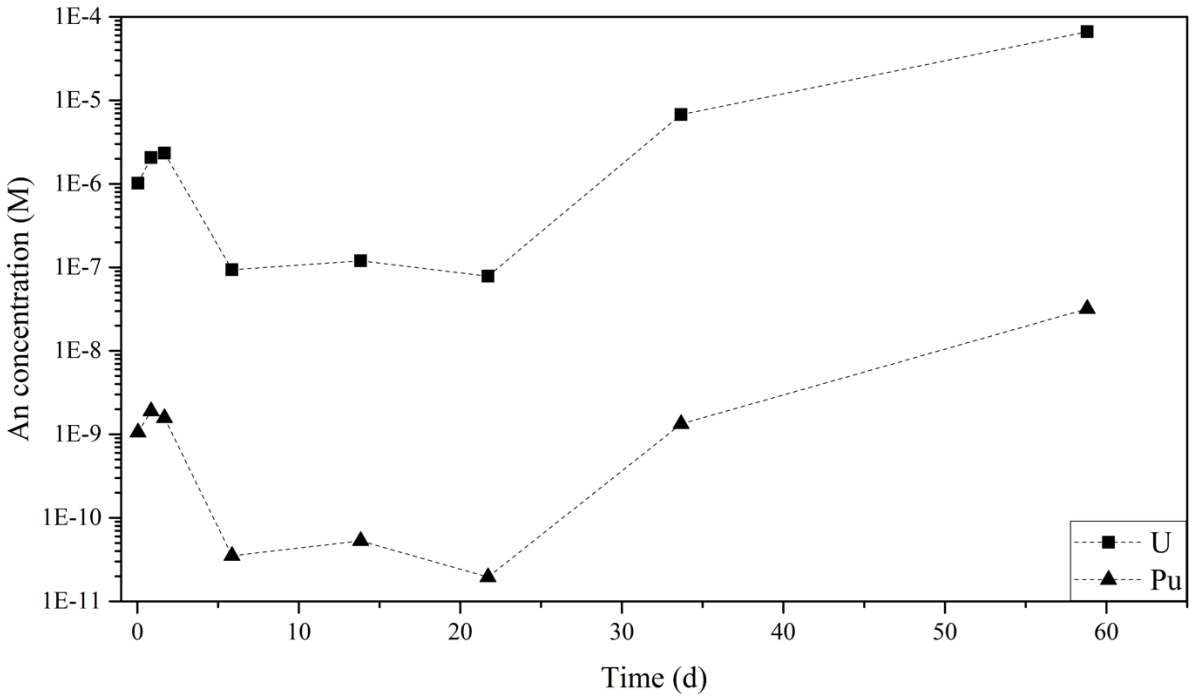

Figure 18. Concentrations of U and Pu in the water during leaching of MOX in an argon atmosphere.

6.7. H_2 activation in the absence of ε-particles

As mentioned previously, the hydrogen effect has often been related to the presence of ε-particles in the spent fuel [79-81]. The results of the MOX leaching clearly confirms that activation of hydrogen does not only occur on the metallic particles, but also on the actinide oxide surface. This is in agreement with previous studies of α-doped fuel [11, 42, 50].

While fuel matrices with metallic inclusions may be of higher relevance for safety assessments, studies of un-irradiated fuel are a necessary complement in order to fully establish the mechanisms of the hydrogen effect. The catalytic properties of light actinides [82] support the possibility of hydrogen activation on uranium or plutonium oxide surfaces. A number of studies have shown indications of a catalytic formation of water by recombination of oxygen and hydrogen on oxidized U metal [83, 84]. However, the presence of water prevents the oxide surface from acting as a basic catalyst [85], hence the role of such catalytic properties of actinide oxides in our experimental conditions is expected to be very limited. On the other hand, water formation and recombination reactions are reported also for α-emitting solids such as ^{244}Cm-doped NpO_2 [86] and PuO_2 [87] surfaces. Such recombination reactions also seem to take place in the MOX experiment presented here, based on the large amounts of HDO analysed.

7. Conclusions

The research presented in this thesis has included studies on homogeneous α-radiolysis, as well as leaching of SIMFUEL and an un-irradiated MOX fuel under repository conditions.

It was shown that the presence of bromide in the groundwater has no effect on the radiolytic production of hydrogen peroxide and oxygen during α-radiolysis. Bromide should therefore not be of any concern in relation to safety assessments dealing with groundwater intrusion in a geological repository at a time when β(γ)-emitting nuclides have decayed.

In addition, the homogeneous radiolysis experiments show that consumption of α-radiolytic oxidants by hydrogen does not occur in the bulk solution. The absence of hydrogen effect observed during homogeneous α-radiolysis confirms the role of fuel surfaces in activating the hydrogen.

Results of the leaching studies suggest that only a very small fraction of the radiolytically produced hydrogen peroxide causes fuel dissolution by oxidation of uranium, whereas the main part decomposes on the fuel surface. Decomposition of the hydrogen peroxide results in the formation of water and oxygen, which is a less reactive oxidant. Alternatively, the hydroxyl radicals formed in the first stage of hydrogen peroxide decomposition react with hydrogen and form water. The proposed second alternative is supported by the formation of semi-heavy water (HDO) during fuel leaching under a deuterium atmosphere, which occurs both in the presence and in the absence of metallic inclusions in the fuel matrix.

Finally, leaching of high activity un-irradiated MOX fuel has shown that the protective effect of hydrogen on radiation-induced oxidative dissolution is maintained even at α-activities comparable to those of fresh spent fuel, and in the absence of ε-particles.

8. Future Work

The results presented in this thesis indicate that a reaction occurs between dissolved hydrogen and hydroxyl radicals from the decomposition of hydrogen peroxide on fuel surfaces. However, in order to completely dismiss other sources for the HDO formation further investigations are necessary. At present the focus lies on elimination of other possible alternatives by analysis of the gas phase. This approach requires quantitative determination of ppm amounts of HD in a background of D_2, which could be technically challenging but well worth attempting.

The unexpected results relating to the high activity MOX leaching further enhances the question of a connection between the hydrogen effect and the α-activity. This is also an area in which continued studies would be of interest.

Acknowledgements

The Swedish Nuclear Fuel and Waste Management Company (SKB) is gratefully acknowledged for the funding of this work.

I would also like to take this opportunity to express my gratitude to all the people who have helped and supported me during my time as a PhD student.

To my supervisors Christian, Kastriot and Patrik, thank you for always being available to give feedback and advice regardless of the time of day, for sharing your knowledge, and for all your support and encouragement throughout these years.

To my examiner Gunnar, thank you for much valued help and advice.

To all the people at NC/IMR who have been my friends and colleagues for the past years – thank you for always being there to give a helping hand, for good company in the lab and for all the fun times during traveling and courses. You will be missed!

In particular, I would like to thank Marcus, who has been working with me from day one, always ready to help out whenever I run into problems or just need someone to discuss with.

Sandra, Artem and Niklas, thank you for being such wonderful office mates. I am also very grateful to Niklas for taking care of lab work during the last months of this project.

Mum, Dad, Jenny, Carl-Johan and Ida, thank you for always believing in me and encouraging me.

Niklas and Mikey – I am so lucky to have you in my life. Thank you for sharing this journey with me.

References

[1] International Atomic Energy Agency. (2016) *Nuclear power reactors in the world*. (IAEA Reference data series No. 2, 2016 Edition).

[2] International Energy Agency. (2016) *Key world energy statistics*.

[3] Svensk Kärnbränslehantering AB. (2010) *Design and production of the KBS-3 repository*. (SKB Technical Report TR-10-12).

[4] Svensk Kärnbränslehantering AB. (2016) *RD&D Programme 2016 – Programme for research, development and demonstration of methods for the management and disposal of nuclear waste*. (SKB Technical Report TR-16-15).

[5] Svensk Kärnbränslehantering AB. (2011) *Long-term safety for the final repository for spent nuclear fuel at Forsmark – Main report of the SR-Site project*. (SKB Technical Report TR-11-01).

[6] Nuclear Energy Agency. (2012) *The post-closure radiological safety case for a spent fuel repository in Sweden – An international peer review of the SKB licence-application study of March 2011 (Final report)*. (NEA/RWM/PEER(2012)2).

[7] Hedin, A. (1997) *Spent nuclear fuel – how dangerous is it? A report from the project "Description of risk"*. (SKB Technical Report TR-97-13).

[8] Shoesmith, D. W. (2000) Fuel corrosion processes under waste disposal conditions. *Journal of Nuclear Materials*, vol. 282, pp. 1-31.

[9] National Cooperative for the Disposal of Radioactive Waste. (2005) *Spent fuel evolution under disposal conditions – Synthesis of results from the EU Spent Fuel Stability (SFS) project*. (NAGRA Technical Report 04-09).

[10] Spahiu, K., Cui, D., Lundström, M. (2004) The fate of radiolytic oxidants during spent fuel leaching in the presence of dissolved near field hydrogen. *Radiochimica Acta*, vol. 92, pp. 625-629.

[11] Carbol, P., Cobos-Sabate, J., Glatz, J.-P., Ronchi, C., Rondinella, V., Wegen, D. H., Wiss, T., Loida, A., Metz, V., Kienzler, B., Spahiu, K., Grambow, B., Quiñones, J., Martinez Esparza Valiente, A. (2005) *The effect of dissolved hydrogen on the dissolution of ^{233}U doped UO_2(s), high burn-up spent fuel and MOX fuel*. (SKB Technical Report TR-05-09).

[12] Pfennig, G., Klewe-Nebenius, H., Seelmann-Eggebert, W. (1998) *Chart of the nuclides*. 6th edition. Lage: Druckhaus Haberbeck.

[13] Choppin, G., Liljenzin, J.-O., Rydberg, J., Ekberg, C. (2013) Principles of nuclear power. In *Radiochemistry and nuclear chemistry, 4th ed*., pp. 595-653. Elsevier Inc.

[14] Loveland, W., Morrissey, D. J., Seaborg, G. T. (2006) Fission. In *Modern nuclear chemistry*, pp. 299-330. Hoboken, New Jersey: John Wiley & Sons, Inc.

[15] Kleykamp, H. (1985) The chemical state of the fission products in oxide fuels. *Journal of Nuclear Materials*, vol. 131, pp. 221-246.

[16] Holm, M. (2011) *RadTox, a computer program for assessing radiotoxicity curves for used nuclear fuel*. Gothenburg: Chalmers University of Technology. (Master's thesis at the Department of Nuclear Chemistry).

[17] International Atomic Energy Agency. (2009) *Classification of radioactive waste*. (IAEA Safety Standards, General Safety Guide No. GSG-1).

[18] Svensk Kärnbränslehantering AB (2017) *Mellanlagret Clab*. http://www.skb.se/anlaggningar-i-drift/mellanlagret-clab/ (2017-03-07).

[19] Sunder, S., Boyer, G.D., Miller N.H. (1990) XPS studies of UO_2 oxidation by alpha radiolysis of water at 100 C, *Journal of Nuclear Materials*, vol. 175, pp. 163-169.

[20] Clark, D. L., Hecker, S. S., Jarvinen, G. D., Neu, M. P. (2006) Plutonium. In *The chemistry of the actinides and transactinide elements*, ed. L. R. Morss, N. M. Edelstein, J. Fuger, J. J. Katz, pp. 813-1264. Dordrecht: Springer Netherlands.

[21] Choppin, G. R., Bond, A. H., Hromadka, P. M. (1997) Redox speciation of plutonium. *Journal of Radioanalytical and Nuclear Chemistry*, vol. 219, issue 2, pp. 203-210.

[22] Krot, N. N., Gel'man, A. D. (1967) Preparation of neptunium(VII) and plutonium (VII). *Doklady Akademii Nauk SSSR*, vol. 177, issue 1, pp. 124-125.

[23] Antonio, M. R., Williams, C. W., Sullivan, J. A., Skanthakumar, S., Hu, Y.-J., Soderholm, L. (2012) Preparation, stability, and structural characterization of plutonium(VII) in alkaline aqueous solution. *Inorganic Chemistry*, vol. 51, issue 9, pp. 5274-5281.

[24] Nikonov, M. V., Gogolev, A. V., Tananaev, I. G., Myasoedov, B. F. (2004). On the highest oxidation states of plutonium in alkali solutions in the presence of ozone. *Radiochemistry*, vol. 46, no. 4, pp. 312-314.

[25] Nikonov, M. V., Gogolev, A. V., Tananaev, I. G., Myasoedov, B. F. (2005) Experimental data points to the existence of plutonium(VIII) in alkaline solutions. *Mendeleev Communications*, vol. 15, issue 2, pp. 50-52.

[26] Tananaev, I. G., Nikonov, M. V., Myasoedov, B. F., Clark, D. L. (2007) Plutonium in higher oxidation states in alkaline media. *Journal of Alloys and Compounds*, vols. 444-445, pp. 668-672.

[27] Nikonov, M. V., Myasoedov, B. F. (2010) Oxidation of Pu(VI) with ozone and stability of the oxidation products, Pu(VII) and Pu(VIII), in concentrated alkali solutions. *Radiochemistry*, vol. 52, no. 1, pp. 17-21.

[28] Rabideau, S. W. (1953) Equilibria and reaction rates in the disproportionation of Pu(IV). *Journal of the American Chemical Society*, vol. 75, issue 4, pp. 798-801.

[29] Madic, C., Begun, G. M., Hobart, D. E., Hahn, R. L. (1984) Raman spectroscopy of neptunyl and plutonyl ions in aqueous solution: Hydrolysis of Np(VI) and Pu(VI) and disproportionation of Pu(V). *Inorganic Chemistry*, vol. 23, issue 13, pp. 1914-1921.

[30] Neck, V., Kim, J. I. (2001) Solubility and hydrolysis of tetravalent actinides. *Radiochimica Acta*, vol. 89, issue 1, pp. 1-16.

[31] Knopp, R., Neck, V., Kim, J. I. (1999) Solubility, hydrolysis and colloid formation of plutonium(IV). *Radiochimica Acta*, vol. 86, issue 3-4, pp. 101-108.

[32] Walther, C., Rothe, J., Brendebach, B., Fuss, M., Altmaier, M., Marquardt, C. M., Büchner, S., Cho, H.-R., Yun, J.-I., Seibert, A. (2009) New insights in the formation process of Pu(IV) colloids. *Radiochimica Acta*, vol. 97, issue 4-5, pp. 199-207.

[33] Ekberg, C., Larsson, K., Skarnemark, G., Ödegaard-Jensen, A., Persson, I. (2013) The structure of plutonium(IV) oxide as hydrolysed clusters in aqueous suspensions. *Dalton Transactions*, vol. 42, pp. 2035-2040.

[34] Brown, P. L., Ekberg, C. (2016) *Hydrolysis of metal ions.* Weinheim: Wiley-VCH. (Volume 1).

[35] Clark, D. L. (2000) The chemical complexities of plutonium. *Los Alamos Science*, no. 26, pp. 364-381.

[36] Krauskopf, K. B. (1986) Thorium and rare-earth metals as analogs for actinide elements. *Chemical Geology*, vol. 55, pp. 323-335.

[37] Reilly, S. D., Runde, W., Neu, M. P. (2007) Solubility of plutonium(VI) carbonate in saline solutions. *Geochimica et Cosmochimica Acta*, vol. 71, pp. 2672-2679.

[38] Kim, J. I. (1993) Chemical behavior of transuranium elements and barrier functions in natural aquifer systems. *Materials Research Society Symposium Proceedings*, vol. 294. pp. 3-21.

[39] Pashalidis, I., Czerwinski, K. R., Fanghänel, T., Kim, J. I. (1997) Solid-liquid phase equilibria of Pu(VI) and U(VI) in aqueous carbonate systems. Determination of stability constants. *Radiochimica Acta*, vol. 76, pp. 55-62.

[40] Choppin, G., Liljenzin, J.-O., Rydberg, J., Ekberg, C. (2013) Radiation effects on matter. In *Radiochemistry and nuclear chemistry, 4th ed.*, pp. 209-238. Elsevier Inc.

[41] Jégou, C., Muzeau, B., Broudic, V., Poulesquen, A., Roudil, D., Jorion, F., Corbel, C. (2005) Effect of alpha irradiation on UO_2 surface reactivity in aqueous media. *Radiochimica Acta*, vol. 93, pp. 35-42.

[42] Muzeau, B., Jégou, C., Delaunay, F., Broudic, V., Brevet, A., Catalette, H., Simoni, E., Corbel, C. (2009) Radiolytic oxidation of UO_2 pellets doped with alpha-emitters ($^{238/239}$Pu). *Journal of Alloys and Compounds*, vol. 467, issues 1-2, pp. 578-589.

[43] Ekeroth, E., Roth, O., Jonsson, M. (2006) The relative impact of radiolysis products in radiation induced oxidative dissolution of UO_2. *Journal of Nuclear Materials*, vol. 355, pp. 38-46.

[44] Jonsson, M. (2010) Radiation-induced processes at solid-liquid interfaces. In *Recent trends in radiation chemistry*, ed. J. F. Wishart, B. S. M. Rao, pp. 301-323. Singapore: World Scientific Publishing Co.

[45] Spahiu, K., Werme, L., Eklund, U.-B. (2000) The influence of near field hydrogen on actinide solubilities and spent fuel leaching. *Radiochimica Acta*, vol. 88, pp. 507.511.

[46] Röllin, S., Spahiu, K., Eklund, U.-B. (2001) Determination of dissolution rates of spent fuel in carbonate solutions under different redox conditions with a flow-through experiment. *Journal of Nuclear Materials*, vol. 297, issue 3, pp. 231-243.

[47] King, F., Shoesmith, D. W. (2004) *Electrochemical studies of the effect of H_2 on UO_2 dissolution*. (SKB Technical Report TR-04-20).

[48] Loida, A., Metz, V., Kienzler, B., Geckeis, H. (2005) Radionuclide release from high burnup spent fuel during corrosion in salt brine in the presence of hydrogen overpressure. *Journal of Nuclear Materials*, vol. 346, pp. 24-31.

[49] Carbol, P., Fors, P., Van Winckel, S., Spahiu, K. (2009) Corrosion of irradiated MOX fuel in presence of dissolved H_2. *Journal of Nuclear Materials*, vol. 392, issue 1, pp. 45-54.

[50] Carbol, P., Fors, P., Gouder, T., Spahiu, K. (2009) Hydrogen suppresses UO_2 corrosion. *Geochimica et Cosmochimica Acta*, vol. 73, issue 15, pp. 4366-4375.

[51] Trummer, M., Roth, O., Jonsson, M. (2009) H_2 inhibition of radiation induced dissolution of spent nuclear fuel. *Journal of Nuclear Materials*, vol. 383, pp. 226-230.

[52] Pastina, B., LaVerne, J. A. (2001) Effect of molecular hydrogen on hydrogen peroxide in water radiolysis. *The Journal of Physical Chemistry A*, vol. 105, pp. 9316-9322.

[53] Trummer, M., Jonsson, M. (2010) Resolving the H_2 effect on radiation induced dissolution of UO_2-based spent nuclear fuel. *Journal of Nuclear Materials*, vol. 396, pp. 163-169.

[54] Spahiu. K., Devoy, J., Cui, D., Lundström, M. (2004) The reduction of U(VI) by near field hydrogen in the presence of UO_2(s). *Radiochimica Acta*, vol. 92, pp. 597-601.

[55] Hochanadel, C. J. (1952) Effects of cobolt γ-radiation on water and aqueous solutions. *Journal of Physical Chemistry*, vol. 56, issue 5, pp. 587-594.

[56] Sworski, T. J. (1954) Yields of hydrogen peroxide in the decomposition of water by cobalt γ-radiation. I. Effect of bromide ion. *Journal of the American Chemical Society*, vol. 76, issue 18, pp. 4687-4692.

[57] Matheson, M. S., Mulac, W. A., Weeks, J. L., Rabani, J. (1966) The pulse radiolysis of deaerated aqueous bromide solutions. *The Journal of Physical Chemistry*, vol. 70, issue 7, pp. 2092-2099.

[58] Zehavi, D., Rabani, J. (1972) The oxidation of aqueous bromide ions by hydroxyl radicals. *The Journal of Physical Chemistry*, vol. 76, issue 3, pp. 312-319.

[59] Behar, D. (1972) Pulse radiolysis studies on Br^- in aqueous solution: The mechanism of Br_2^- formation. *The Journal of Physical Chemistry*, vol. 76, issue 13, pp. 1815-1818.

[60] Mamou, A., Rabani, J., Behar, D. (1977) On the oxidation of aqueous Br^- by OH radicals, studied by pulse radiolysis. *The Journal of Physical Chemistry*, vol. 81, issue 15, pp. 1447-1448.

[61] LaVerne, J. A., Ryan, M. R., Mu, T. (2009) Hydrogen production in the radiolysis of bromide solutions. *Radiation Physics and Chemistry*, vol. 78, pp. 1148-1152.

[62] Metz, V., Bohnert, E., Kelm, M., Schild, D., Reinhardt, J., Kienzler, B., Buchmeiser, M. R. (2007) *Materials Research Society Symposium Proceedings*, vol. 985, pp. 33-40.

[63] Metz, V., Loida, A., Bohnert, E., Schild, D., Dardenne, K. (2008) Effects of hydrogen and bromide on the corrosion of spent nuclear fuel and γ-irradiated UO_2(s) in NaCl brine. *Radiochimica Acta*, vol. 96, pp. 637-648.

[64] Crumière, F., Vandenborre, J., Essehli, R., Blain, G., Barbet, J., Fattahi, M. (2013) LET effects on the hydrogen production induced by the radiolysis of pure water. *Radiation Physics and Chemistry*, vol. 82, pp. 74-79.

[65] Lucuta, P. G., Verrall, R. A., Matzke, Hj., Palmer, B. J. (1991) Microstructural features of SIMFUEL – Simulated high-burnup UO_2-based nuclear fuel. *Journal of Nuclear Materials*, vol. 178, pp. 48-60.

[66] Nitsche, H., Lee, S. C., Gatti, R. C. (1988) Determination of plutonium oxidation states at trace levels pertinent to nuclear waste disposal. *Journal of Radioanalytical and Nuclear Chemistry*, vol. 124, issue 1, pp. 171-185.

[67] Choppin, G. R., Bond, A. H., Hromadka, P. M. (1997) Redox speciation of plutonium. *Journal of Radioanalytical and Nuclear Chemistry*, vol. 219, issue 2, pp. 203-210.

[68] Allen, A. O., Hochanadel, C. J., Ghormley, J. A., Davis, T. W. (1952) Decomposition of water and aqeous solutions under mixed fast neutron and gamma radiation. *Journal of Physical Chemistry*, vol. 56, issue 5, pp. 575-586.

[69] Ghormley, J. A., Stewart, A. C. (1956) Effects of γ-radiation on ice. *Journal of the American Chemical Society*, vol. 78, issue 13, pp. 2934-2939.

[70] International Atomic Energy Agency. (2009) *Laser spectroscopic analysis of liquid water samples for stable hydrogen and oxygen isotopes*. (IAEA Training course series No. 35).

[71] Jouzel, J. (2011) Water stable isotopes: Atmospheric Composition and applications in polar ice core studies. In *Isotope geochemistry – From the treatise on geochemistry*, ed. H. D. Holland, K. K. Turekian, pp. 151-180. Elsevier Ltd.

[72] Kienzler, B., Loida, A., González-Robles, E., Müller, N., Metz, V. (2014) Fast/instant radionuclide release: Effects inherent to the experiment. *Materials Research Society Symposium Proceedings*, vol. 1665, pp. 233-243.

[73] Loida, A., Metz, V., Kienzler, B. (2007) Alteration behavior of high burnup spent fuel in salt brine under hydrogen overpressure and in presence of bromide. *Materials Research Society Symposium Proceedings*, vol. 985, pp. 15-20.

[74] Ödegaard-Jensen, A., Fors, P. A. Ödegaard-Jensen *et al*., EU-project NF-PRO FI6W-CT-2003-02389 D-No:1.5.17, 2008.

[75] Cui, D., Ekeroth, E., Fors, P. Spahiu, K. (2008) Surface mediated processes in the interaction of spent fuel or α-doped UO_2 with H_2. *Materials Research Society Symposium Proceedings*, vol. 1104, pp. 112-124.

[76] Sander, R. (2015) Compilation of Henry's law constants (version 4.0) for water as solvent. *Atmospheric Chemistry and Physics*, vol. 15, pp. 4399-4981.

[77] Sellin, P. (2001) SR 97: Hydromechanical evolution in a defective canister. *Materials Research Society Symposium Proceedings*, vol. 663, pp. 755-763.

[78] Bonin, B., Colin, M., Dutfoy, A. (2000) Pressure building during the early stages of gas production in a radioactive waste repository. *Journal of Nuclear Materials*, vol. 281, pp. 1-14.

[79] Broczkowski, M. E., Noël, J. J., Shoesmith, D. W. (2005) The inhibiting effects of hydrogen on the corrosion of uranium dioxide under nuclear waste disposal conditions. *Journal of Nuclear Materials*, vol. 346, pp. 16-23.

[80] Jonsson, M., Nielsen, F., Roth, O., Ekeroth, E., Nilsson, S., Hossain, M. M. (2007) Radiation induced spent nuclear fuel dissolution under deep repository conditions. *Environmental Science & Technology*, vol. 41, pp. 7087-7093.

[81] Eriksen, T., Shoesmith, D. W., Jonsson, M. (2012) Radiation induced dissolution of UO_2 based nuclear fuel – A critical review of predictive modelling approaches. *Journal of Nuclear Materials*, vol. 420, pp. 409-423.

[82] Colmenares, C. A. (1984) Oxidation mechanisms and catalytic properties of the actinides. *Progress in Solid State Chemistry*, vol. 15, issue 4, pp. 257-364.

[83] Baker, M. McD., Less, L. N., Orman, S. (1966) Uranium + water reaction. Part 1. – Kinetics, products and mechanism. *Transactions of the Faraday Society*, vol. 62, pp. 2513-2524.

[84] Baker, M. McD., Less, L. N., Orman, S. (1966) Uranium + water reaction. Part 2. – Effect of oxygen and other gases. *Transactions of the Faraday Society*, vol. 62, pp. 2525-2530.

[85] Hattori, H. (1995) Heterogeneous basic catalysis. *Chemical Reviews*, vol. 95, pp. 537-558.

[86] Icenhour, A. S., Toth, L. M., Wham, R. M., Brunson, R. R. (2004) A simple kinetic model for the alpha radiolysis of water sorbed on NpO_2. *Nuclear Technology*, vol. 146, pp. 206-209.

[87] Haschke, J. M., Allen, T. H., Stakebake, J. L. (1996) Reaction kinetics of plutonium with oxygen, water and humid air: moisture enhancement of the corrosion rate. *Journal of Alloys and Compounds*, vol. 243, pp. 23-35.

List of Abbreviations

BWR	Boiling water reactor
CLAB	Centralt mellanlager för använt kärnbränsle och högaktiva reaktordelar (Central interim storage facility for spent nuclear fuel)
C-SEM	Continuous secondary electron multiplier
EW	Exempt waste
HLW	High level waste
HPGe	High purity germanium
HTTA	2-theonyl-trifluoro acetone
ICP-MS	Inductively coupled plasma mass spectrometry
ILW	Intermediate level waste
KBS-3	Method for disposal of used nuclear fuel developed by SKB (Swedish Nuclear Fuel and Waste Management Co.)
LET	Linear energy transfer
LSC	Liquid scintillation counting
LLW	Low level waste
MOX	Mixed oxide
PWR	Pressurized water reactor
SEM	Secondary electron multiplier
SFL	Slutförvar för långlivat radioaktivt avfall (Final repository for long-lived radioactive waste)
SFR	Slutförvar för kortlivat radioaktivt avfall (Final repository for short-lived radioactive waste)
SIMFUEL	Simulated high-burnup nuclear fuel
SMOW	Standard mean ocean water
VLLW	Very low level waste
VSLW	Very short-lived waste